Studies on the Selenium Barrier Layer Photoelement. VI.

Abnormal Spectral Sensibility of a Selenium Barrier Layer Photoelement.

By Masao TOMURA.

(Received November 10, 1948.)

Introduction. The author has explained the mechanism of the barrier layer photoelement and rectification of the selenium barrier layer cell, by considering its barrier layer which is made at the contact between a metal and selenium semiconductor.(1) According to him, the barrier layer is one in which the distribution of electrons is abnormal and there exists a very large internal field. If the incident light is absorbed in the barrier layer, photoelectrons and their holes which are created by the internal photoeffect of selenium cause a photocurrent in the external circuit owing to the acceleration by the internal field. On the other hand, the existence of the barrier layer gives the action of rectification to the photoelement.

The barrier layer of a normal selenium barrier layer cell is composed of the selenium semiconductor itself. In order to study the structure of the layer and the mechanism of the barrier layer photoeffect and rectification, it is desirable to make a barrier layer which is different chemically from selenium.

Description of Experiments. After the coating of the melted selenium on a metal base electrode, it is converted to a semiconductor by the heat treatment of 4 hours at 200°C and then a thin cadmium film is deposited on it by the cathode sputtering method in the atmosphere of argon. In the next place, after the second heat treatment of 4 hours at 200°C in vacuum, a translucent platinum electrode is put on the element by the cathode sputtering.

The spectral sensibility of the element is measured by a monochrometer over the range of 4000 Å~8000 Å. The result is shown in Fig. 1. It shows a new peak of 7100Å besides the one of a normal cell. The relative height of the new peak with respect to the normal one increases with the thickness of the sputtered cadmium film. The curves 1, 2, 3 in Fig. 1 are spectral distributions of the samples of which the thickness of the cadmium film increases in that order. The thickness of the sputtered film is in the order of 1~10 mμ.

(1) M. Tomura, *Proc. Toshiba. Lab.*, **18** (1943), 523.

If the heat treatment is omitted after the deposition of the cadmium film, we can observe no new peak of spectral sensibility.

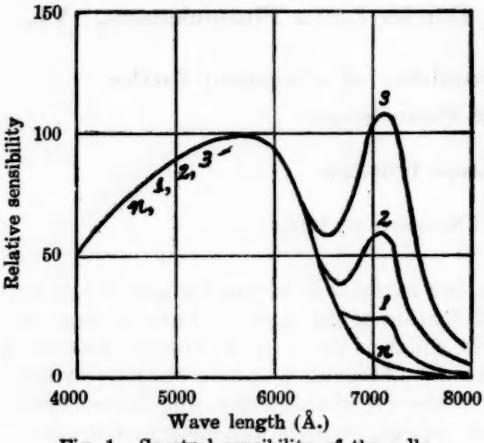

Fig. 1. Spectral sensibility of the cells. The curve n is one of a normal cell.

To have knowledge of the change of the rectification by the heat treatment, another sample is made which has a thick cadmium film evaporated in vacuum on the selenium semiconductor. Its static characteristics of rectification are measured before and after the heat treatment of 1 hour at 100°C. The result is shown in Fig. 2. The resistance of the barrier layer becomes very large by the heat treatment.

On the other hand, to see what substance is created on the selenium by the heat treatment, a direct method of detection utilizing the reflection method of electron diffraction was used for a sample which was made by the heat treatment of 4 hours at 200°C in vacuum. As usual the cadmium film of the order of 10 $m\mu$ thick was deposited on the selenium semiconductor by evaporating in vacuum before the heat treatment. The result of the electron diffraction shows the existence of a CdSe layer of the zinc blend type.

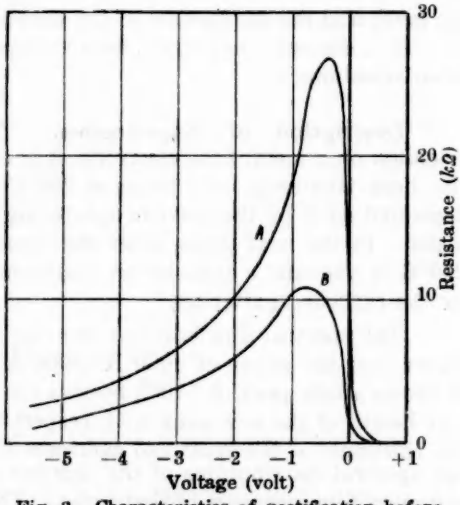

Fig. 2. Characteristics of rectification before (B) and after (A) the heat treatment.

Next, the author measured the spectral transmission of CdSe which was deposited on a glass plate by the vacuum evaporation. This CdSe was made by the wet method, namely, by using the reaction of $Cd^{++} + H_2Se \rightarrow CdSe + 2H^+$. The transmission curve is in Fig. 3.

Discussion of the Experiments. It is clear that the new peak of 7100 Å is caused by the heat treatment. The author has already explained the process of the reaction of cadmium and selenium semiconductor by

finding a thermoionic current occurring at a contact of both materials.[2] By the increase of the mobility owing to high temperatures, cadmium ions

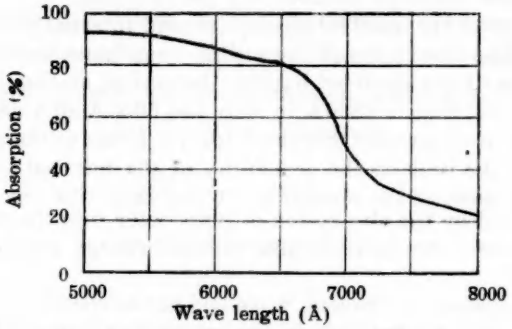

Fig. 3. Absorption spectrum of CdSe film.

accelerated by the internal field move through the CdSe layer at the contact and the layer of CdSe grows with the flowing of ionic current in the external circuit. This means just the converting process of the free energy difference in the reaction $Cd+Se \rightarrow CdSe$ into the electric energy.

The fact that the CdSe layer is found on the selenium by the electron diffraction tells us that the entire layer of the cadmium deposited on the selenium has reacted with the selenium.

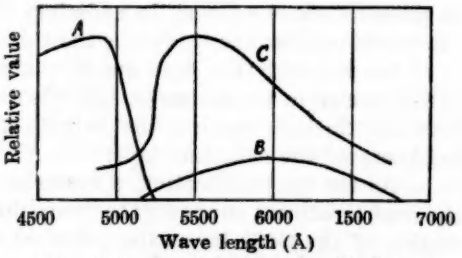

Fig. 4 (b). Spectral absorption (A, B) and photoconductivity (C) of CdS[9].

In this way the barrier layer of the new photoelement is composed of double layers; the CdSe layer and selenium layer over which the internal field extends. If the light is put on the layer, it is first absorbed in the CdSe layer and next in the selenium layer. Then the normal peak of the spectral sensibility is attributed to the internal photoeffect of the selenium and the new peak of 7100 Å to the one of the CdSe layer.

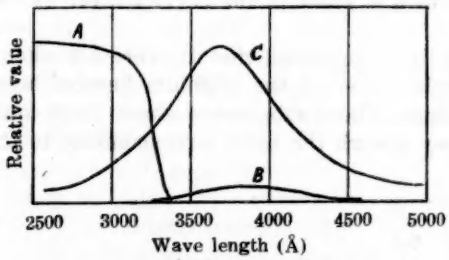

Fig. 4 (a). Spectral absorption (A, B) and photoconductivity (C) of Zn_2S[9].

It has been reported that CdSe has the internal

(2) M. Tomura, this Bulletin, 22 (1949), 82.

photoeffect.[3] From the spectral sensibility of the internal photoeffect and spectral absorption of ZnS and CdS, the following hypothesis to explain the barrier layer photoeffect of CdSe is given.

Fig. 4 shows the spectral absorption and internal photoeffect of ZnS and CdS.[4] The absorption in the visible range corresponds to the transition of electrons from the filled band to the excited states. The tails of the absorption curve, that is 3800Å of ZnS and 6000Å of CdS, correspond to the transition of electrons from the impurity levels to their excited states. The fact that the peak of the sensibility of the internal photoeffect coincides with the peak of the absorption by the impurities means that photoelectrons excited by the absorption of light enter into the conduction band from the excited states by absorbing thermal energy and contribute to the conduction.[5]

From the shape of the long wave end of the spectral absorption curve of CdSe measured by the author, we presume that the characteristic absorption of CdSe extends to the region of the absorption curve by the impurity centre. Consequently the internal photoeffect is expected at the long wave end as well as ZnS and CdS.

As the heat treatment is long enough in duration and high enough in temperature to convert the cadmium film to the CdSe layer; the thicker the cadmium film, the thicker is the CdSe layer formed.

Consequently the light quantity absorbed in the CdSe layer becomes greater relative to the one in the selenium layer when the cadmium film becomes thicker, making the height of the new peak higher with the thickness of the cadmium layer.

As for the rectification, a remarkable change of the resistance after the heat treatment supports the formation of the CdSe layer. By the formation of the CdSe layer, the potential hill to the stream of the positive hole becomes higher at the contact, resulting in the increase of the resistance of the barrier layer.

Conclusions. A selenium barrier layer photoelement which has a new process of heat treatment in its making is formed, having a new peak in its spectral sensibility curve. This peak is attributed to the internal photoeffect of the CdSe layer which is made in the barrier layer by the heat treatment.

From the above discussions, it is concluded that if there are photoconductive substances in the barrier layer of the selenium barrier layer cell where the internal field influences, these substances show their own barrier layer photoeffect when they absorb the light corresponding to the internal photoeffect.

Matsuda Research Laboratory of
the Tokyo Shibaura Electric Co., Ltd.

(3) R. Freirchs, *Phys. Rev.*, **72** (1947), 594.
(4) J. H. Gisolf, *Physica*, **6** (1939), 81; F. A. Kröger, ibid., **7** (1940), 1; B. Gudden and R. W. Pohl, *Z. Physik*, **2** (1920), 181.
(5) F. Seitz, *J. Chem. Phys.*, **6** (1938), 454.

On the Equilibrium of the Radioactive Elements in the Hydrosphere. V.[1] A Simple Method for Distinguishing Uranium and Thorium in Radioactive Minerals.

By Kazuo KURODA

(Received November 16, 1948.)

It was found that the uranium and thorium in radioactive minerals are easily distinguished by measuring the radioactivity of radium emanation and thorium emanation in the minerals. Though this method is a qualitative one, it may be improved in future and it will be used as a quantitative method for determining the ratio of uranium to thorium in radioactive minerals.

Method of Experiment. Several grams of powdered minerals are taken in a vessel, and 50 to 100 c.c. of water are added. The radioactivity of the water is measured on the next day. The water is taken with an injector (about 50 c.c.), as quickly as possible, and the radioactivity is measured at once. In the case of thorium minerals, a rapid decay curve of thorium emanation will be obtained and in th ecase of uranium minerals, on the other hand, the radioactivity will increase gradually as the result of the formation of the decay products of the radium emanation. In the case of radioactive minerals containing both series of radioactive elements, the radioactivity of radium emanation and thorium emanation will be simultaneously observed.

Results of Experiment. (a) Pitchblende. The powdered sample of pitchblende (about 3 grams) was immersed in distilled water (about 50 c.c.) overnight. A 20 c.c. portion of the water was taken with an injector, as quickly as possible, and it was ejected in the ionization chamber of I.M. fontactoscope. The radioactivity measurement was commenced at once. An example of the experiments is shown in Table 1.

Table 1. Pitchblende.

Time (min.)	Radioactivity (div./min.)
1	7.7
2	7.3
3	9.0
4	9.5
5	10.5
6	13.5
7	13.0
16	16.7
17	17.0

The concentration of radium emanation in the water was calculated to be about 300 Mache. The radioactivity of thorium emanation

(1) Previous Paper. IV. K. Kuroda and Y. Yokoyama, this Bulletin, **22** (1949), 43.

was not observed, as the thorium content of pitchblende was low usually.

(b) Monazite. The powdered sample of monazite (10 grams) was immersed in the distilled water overnight. A 45 c.c. portion of the water was taken with an injector, as quickly as possible, and it was ejected in the ionization chamber of I.M. fontactoscope. The radioactivity measurement was commenced at once, and the following result was obtained (Table 2).

Table 2. Monazite.

Time (min.)	Radioactivity (div./min.)
1	2.4
2	1.2
3	0.8
4	0.8
5	0.5
6	0.7
7	0.4
8	0.6
9	0.7
10	0.4

Table 2 shows that the thorium emanation dissolves out from the mineral, but the radium emanation does not.*) The concentration of thorium emanation in the water is calculated to be about 30 Tn-Mache.

(c) Enalite. The thorium content of this mineral is about 55 per cent and the uranium content is about 25 per cent. Therefore, it may be expected that both thorium emanation and radium emanation will dissolve out from this mineral, when it is treated as described above.

The powdered sample of enalite (about 40 grams) was immersed in the distilled water (100 c.c.) overnight. A 70 c.c. portion of the water was taken with an injector, and it was ejected in the ionization chamber of I.M. fontactoscope. The result of the experiment is shown in Table 3.

Table 3. Enalite.

Time (min.)	Radioactivity (div./min.)
1	3.6
2	2.0
3	1.4
4	1.7
5	1.7
10	1.6
11	1.6
12	1.9
13	1.7
34	2.0
35	2.1
36	2.1
37	2.4

The concentration of thorium emanation in the water is about 40 Tn-Mache and that of radium emanation is about 10 Mache.

Summary.

It was found that the uranium and thorium in radioactive mineral are easily distinguished by measuring the radioactivity of radium emanation and thorium emanation in the minerals with I.M. fontactoscope.

The author expresses his hearty thanks to Professor Kenjiro Kimura for his kind guidance. The cost of this research was defrayed from the Scientific Research Encouragement Grant from the Department of Education, to which the author's thanks are due.

Chemical Institute, Faculty of Science,
Tokyo University.

*) Natural leak is about 0.5 div./min.

On the Diamagnetism of Perylene. II*.

By Genjiro HAZATO

(Received November, 17, 1948.)

In a preceding paper,[1] we have shown a simple method to compute the diamagnetic anisotropy of aromatic molecules from the experimental values of powdered crystals, and we have found that perylene molecule has an anisotropic part about twice as large as that of naphthalene.

In general, aromatic molecules show abnormally large diamagnetic anisotropy, the susceptibility being maximum if the direction of the impressed field is perpendicular to the molecular plane, and minimum if the two are parallel with each other. To explain this phenomenon, it was assumed by several authors[2] that in these molecules the diamagnetic currents might circulate from one atom to the other along the aromatic ring system. In other words, at each carbon atom, constituting the aromatic ring system, there is a π- or p_z-electron which is free to move, under the influence of the magnetic field, from one carbon atom to the adjacent one. This is closely analogous to the electric current induced in a conducting network. This hypothesis has come to be generally accepted in qualiative explanations.

Starting from the above consideration, quantitative interpretations of the anisotropic parts of the aromatic molecules have been worked out by Pauling[3] and by London[4]. Pauling's argument is based essentially on classical ideas, assuming that the aromatic rings should behave like supraconductors.[5] London uses a quantum mechanical procedure, based on Hückel's molecular orbital treatment, extending to the case of the presence of a magnetic field. He calculated the ratios of the anisotropies of various condensed aromatic compounds to that of benzene, obtaining excellent agreement with experiment.

Here, in this paper, we shall apply the London theory to the theoretical calculation of the anisotropic part of perylene molecule, seeing how far the theory can carry us. The present calculation follows, for convenience' sake, the same notation and procedure as London's paper.[4]

London's secular equation is as follows:

$$| \eta_{kl} \exp(2\pi i f_{kl}) - x\,\delta_{kl} | = 0 \qquad (1)$$

Here η_{kl} $\begin{cases} 1 \text{ if } k \text{ is a neighbor of } l \\ 0 \text{ if } k \text{ is not a neighbor of } l \end{cases}$ δ_{kl} $\begin{cases} 1 \text{ if } k = l \\ 0 \text{ if } k \neq l, \end{cases}$

*) This paper was read at the annual meeting of the chemical constitution of the Chem. Soc. of Japan in Oct. 1946 and in Apr. 1948.

(1) H. Shiba, and G. Hazato, this Bulletin, **22** (1949), 92.

(2) P. Ehrenfest, *Physica*, **5** (1925), 388; *Z. Phys.*, **58** (1929), 719; C. V. Raman, and K. S. Krishnan, *Proc. Roy. Soc. (London)*, **A, 113** (1927), 511; C. V. Raman, *Nature*, **123** (1929), 945; K. Lonsdale, *Proc. Roy, Soc. (London)*, **A. 159** (1937), 149.

(3) L. Pauling, *J. Chem. Phys.*, **4** (1936), 673.

(4) E. London, *J. du Physique*, **8** (1937), 397.

(5) Cf. F. London, *J. Chem. Phys.*, **5** (1937), 837.

and $$x = \frac{E^{(1)} - W_0}{W_1} \qquad (2)$$

$E^{(1)}$ is the ordinary first order perturbation energy:

$$E^{(1)} = E - E^{(0)}, \qquad (3)$$

$E^{(0)}$ is the energy of the zeroth order approximation under the influence of the magnetic field, which is expressed by

$$E^{(0)} = E^{(00)} + \frac{1}{2}\chi H^2, \qquad (4)$$

where χ is the susceptibility contribution of the π-electron (one per aromatic carbon atom), and H is the field strength. In equation (2), W_0 is the Coulomb integral independent of the magnetic field, W_1 is the ordinary exchange integral of the nearest neighbors of the orbital theory in the absence of the magnetic field, and in this case, this is used as a unit of the energy scale. In equation (1),

$$\exp(2\pi i f_{kl}) = W_{kl}/W_1 \qquad (5)$$

and $$f_{kl} = (e/hc)\, H \cdot S_{kl}, \qquad (6)$$

in which W_{kl} represents the exchange integral in the presence of the magnetic field, S_{kl} is the area of the triangle formed by the neighbors k, l and the origin, arbitrarily chosen in the plane of the molecule, therefore, f_{kl} can be considered as a numerical value proportional to the magnetic flux.

Following the above conditions and the model shown in Fig. 1, the secular determinant of perylene molecule can be arranged in the form

$$\begin{array}{c|cccccccccccccccccccc|}
 & 0 & 1 & 2 & 3 & 4 & 0' & 4' & 3' & 2' & 1' & \bar{1}' & \bar{2}' & \bar{3}' & \bar{4}' & \bar{0}' & \bar{4} & \bar{3} & \bar{2} & \bar{1} & \bar{0} & \\
0 & -x & \varepsilon_1^* & & & & 1 & & & & \varepsilon_1 & & & & & & & & & & & \\
1 & \varepsilon_1 & -x & 1 & & & & & & & & & & & & & & & & a\varepsilon_1^* & & \\
2 & & 1 & -x & \varepsilon_2 & & & & & & & & & & & & & & & & & \\
3 & & & \varepsilon_2^* & -x & \varepsilon_3 & & & & & & & & & & & & & & & & \\
4 & & & & \varepsilon_3^* & -x & \varepsilon_2 & & & & & & & & & & & & & & & \\
0' & 1 & & & & \varepsilon_2^* & -x & \varepsilon_2 & & & & & & & & & & & & & & \\
4' & & & & & & \varepsilon_2^* & -x & \varepsilon_3 & & & & & & & & & & & & & \\
3' & & & & & & & \varepsilon_3^* & -x & \varepsilon_2 & & & & & & & & & & & & \\
2' & & & & & & & & \varepsilon_2^* & -x & 1 & & & & & & & & & & \\
1' & \varepsilon_1^* & & & & & & & & 1 & -x & a\varepsilon_1 & & & & & & & & & & \\
\bar{1}' & & & & & & & & & a\varepsilon_1^* & -x & 1 & & & & & & & & & \varepsilon_1 & \\
\bar{2}' & & & & & & & & & & 1 & -x & \varepsilon_2 & & & & & & & & & \\
\bar{3}' & & & & & & & & & & & \varepsilon_2^* & -x & \varepsilon_3 & & & & & & & & \\
\bar{4}' & & & & & & & & & & & & \varepsilon_3^* & -x & \varepsilon_2 & & & & & & & \\
\bar{0}' & & & & & & & & & & & & & \varepsilon_2^* & -x & \varepsilon_2 & & & & 1 & & \\
\bar{4} & & & & & & & & & & & & & & \varepsilon_2 & -x & \varepsilon_3 & & & & & \\
\bar{3} & & & & & & & & & & & & & & & \varepsilon_3^* & -x & \varepsilon_2 & & & & \\
\bar{2} & & & & & & & & & & & & & & & & \varepsilon_2^* & -x & 1 & & & \\
\bar{1} & & a\varepsilon_1 & & & & & & & & & & & & & & & & 1 & -x & \varepsilon_1^* & \\
\bar{0} & & & & & & & & & & & \varepsilon_1^* & & & & 1 & & & & \varepsilon_1 & -x & \\
\end{array} = 0, \qquad (7)$$

in which $\varepsilon=\exp(2\pi i f_{kl})$ and $\varepsilon^*=\exp(-2\pi i f_{kl})$. For convenience' sake, we may prefer ε to ε^*, in case of the clockwise rotation about the center of the central hexagon.

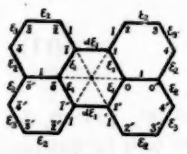

Fig. 1.

The determinant is of even degree in x, and it follows that the roots of x occur in pairs of type $\pm x$. It also follows that, as we see in Fig, 1, the model has symmetrical operation of inversion at the center of the central hexagon. In such a case, the determinant can be tansformed in general to one of the type

$$\begin{vmatrix} \Delta_1 & 0 \\ 0 & \Delta_2 \end{vmatrix} = 0.$$

Accordingly, equation (7) can be separated into the solution of two determinants, namely

$$\Delta_1 = \begin{vmatrix} -x & \varepsilon_1^* & 1 & & & & & \varepsilon_1 \\ \varepsilon_1 & -x & 1 & & & & & a\varepsilon_1^* \\ & 1 & -x & \varepsilon_2 & & & & \\ & & \varepsilon_2^* & -x & \varepsilon_3 & & & \\ & & & \varepsilon_3^* & -x & \varepsilon_2 & & \\ 1 & & & & \varepsilon_2^* & -x & \varepsilon_2 & \\ & & & & & \varepsilon_2^* & -x & \varepsilon_3 \\ & & & & & & \varepsilon_3^* & -x & \varepsilon_2 \\ & & & & & & & \varepsilon_2^* & -x & 1 \\ \varepsilon_1^* & a\varepsilon_1 & & & & & & & 1 & -x \end{vmatrix} = 0 \quad \Delta_2 = \begin{vmatrix} -x & 1 & & & & & & -a\varepsilon_1^* & \varepsilon_1 \\ 1 & -x & \varepsilon_2 & & & & & & \\ & \varepsilon_2^* & -x & \varepsilon_3 & & & & & \\ & & \varepsilon_3^* & -x & \varepsilon_2 & & & & \\ & & & \varepsilon_2^* & -x & \varepsilon_2 & & 1 & \\ & & & & \varepsilon_2^* & -x & \varepsilon_3 & & \\ & & & & & \varepsilon_3^* & -x & \varepsilon_2 & \\ & & & & & & \varepsilon_2^* & -x & 1 \\ -a\varepsilon_1 & & & & & & & 1 & -x & \varepsilon_1^* \\ \varepsilon_1^* & & 1 & & & & & & \varepsilon_1 & -x \end{vmatrix} = 0.$$

Expanding Δ_1 or Δ_2, and after some approximation,[4] we have

$$(x^2-1)\{x^8-10x^6+31x^4-34x^2+9-a^2(x^6-6x^4+8x^2)\mp 2a(x^5-5x^3+7x)\} + \frac{1}{4}(2\pi f)^2\{8x^4-24x^2+24\pm a(x^7-6x^5+28x^3-15x)\} = 0. \quad (8)$$

Where $$f = (e/hc)\cdot H\cdot S_H, \quad (9)$$

S_H = the area of each hexagon.

In equations (7), (8) and in Fig. 1, a is a parameter which can take on the fractional values from zero to 1. That is, if $a=1$, all the hexagons are equally regular ones, and the method is identical with London's general procedure, but in the case of $a=0$, both $1\bar{1}$ and $1'\bar{1}$ (Fig. 1) are pure single bonds, generally speaking, aW_1 represents the exchange integral in $1\bar{1}$, or $1'\bar{1}'$ bond, and in the other places, we can put it equally as W_1 whose value is the same as that of the benzene ring.

Now let x_p be a root of equation (8). From the relation (2) we have

$$E_p^{(1)} = W_0 + x_p W_1. \quad (10)$$

Substituting (4) in (3), and by means of the partial differentiation with regard to H, a susceptibility contribution of a π-electron becomes

$$\chi_p = -\left(\frac{\partial^2 E^{(1)}}{\partial H^2}\right)_{H\to 0}. \tag{11}$$

Since equation (8) has the form: $F_1(x)+(2\pi f)^2 \cdot F_2(x)=0$, let x' be a root of $F_1(x)=0$, and the corresponding root of (8) will be expressed approximately by

$$x = x' + x''(2\pi f)^2, \tag{12}$$

in which

$$x'' = \frac{F_2'(x')}{F_1'(x')},$$

F_1' represents the first derivative of F_1 with regard to x.

From (9), (10), (11) and (12), we obtain London's final result:

$$\Delta\chi = 2\sum_{p=-\frac{N-2}{4}}^{\frac{N-2}{4}} \chi_p = -4\sum(x'') \mid W_1 \mid \left(\frac{2\pi e S_B}{hc}\right)^2. \tag{13}$$

Here, the half of the lowest levels is completely occupied by all the electrons in question, so that each level may be occupied by a pair of electrons, each pair having antiparallel spin directions.

In equation (13), we can take both W_1 and S_B as constants throughout the model constructed by the same regular hexagons. But, in the present case, as is the case with Fig. 1 or equation (8), the area S_B of the central hexagon would be somewhat affected by a, that is, the distance $1\bar{1}$ or $1'\bar{1}'$ would be a function of a; the smaller the value of a becomes, the larger the S_B becomes. In spite of this fact, as it will be shown in a later paper, there is enough reason why we can ignore the S_B-effect of the central hexagon. Consequently, assuming W_1 and S_B to be constants, $\Delta\chi$ must directly be proportional to $\Sigma(x'')$; moreover, even if we take the parameter a as a variable, the corresponding values of $\Sigma(x'')$ may depend almost entirely upon the values of a only.

Now, all we have to do is to compute each numerical value of $\Sigma(x'')$ for each value of a. The solutions of equation (8) are shown in Table 1.

The notation x''' in the table represents the corresponding value of x'' in the case of the presence of non-orthogonality of 25% between the adjacent atomic wave functions, being computed by means of the approximate method of Brooks[6]. In the case of naphthalene each value of

(6) H. Brooks, *J. Chem. Phys.*, **9** (1941), 463.

Table 1.

$\alpha = 0.3$		$\alpha = 0.4$		
$-x'$	x''	$-x'$	x''	x'''
0.51728	+0.2552	0.48745	+0.2312	+0.1837
0.73243	+0.5751	0.77230	+0.6983	+0.4905
1	−0.2564	1	−0.2381	−0.1524
1	−0.4762	1	−0.5555	−0.3555
1.20736	+0.0085	1.17607	−0.0626	−0.0373
1.39765	+0.4770	1.42843	+0.6431	+0.3492
1.58274	−0.3989	1.57327	−0.5625	−0.2897
1.66759	−0.0008	1.68842	+0.0340	+0.0168
2.25520	+0.0142	2.24194	+0.0060	+0.0024
2.36492	+0.0437	2.38958	+0.0463	+0.0182
Σ; 13.725	+0.2414	Σ; 13.757	+0.2402	+0.2259

$\alpha = 0,8$			$\alpha = 1,0$	
$-x'$	x''	x'''	$-x'$	x''
0.38709	+0.1656	+0.1377	0.34729	+0.1442
0.92925	+2.4810	+1.6337	1	0
1	−0.1852	−0.1185	1	−0.1666
1	−1.6666	−1.0666	1	$-\infty$
1.05604	−0.8037	−0.5030	1	$-\infty$
1.54312514133	+349.0068	+181.7375	1.53209	+1.7428
1.54341698022	−348.9217	−181.6741	1.59357	−1.6544
1.80125	+0.1517	+0.0721	1.87938	+0.2176
2.19881	−0.0456	−0.0190	2.18194	−0.0983
2.51173	+0.0512	+0.0193	2.58836	+0.0509
Σ; 13.97	+0.2335	+0.2191	Σ; 14.122	$-\infty$

$\Sigma(x'')$ and $\Sigma(x''')$ amounts to 0.1214[4] and 0.1144[6] respectively. Thus, we have in Table 2 the relative anisotropies of perylene, with regard to a, taking naphthalene as a unit.

Table 2.

α	0.0	0.3	0.4	0.8	1.0
$\Delta\chi$ (pery.)/$\Delta\chi$ (naph.)					
in orthogonal	2.0	1.99	1.97_8	1.92	$-\infty$
in non-orthogonal	2.0	—	1.97_6	1.91_8	$-\infty$
$\Sigma(-x')$	13.68	13.72	13.76	13.97	14.12

We can see from Table 2 that the effect of non-orthogonality is negligibly small.[7]

The results in Table 2 are graphically shown in Fig. 2, from which we obtain the following conclusions:

(7) cf. reference (6).

1. In case of $\alpha=1$, $\Sigma(x'')$ has no definite value.
2. The increase in value of α is accompanied by the increasing of the double bond character in $1\bar{1}$- or $1'\bar{1}'$-bond, and at the same time the total binding energy between the corresponding π-electrons, viz. $2\Sigma(-x')$ increases. This result is a matter of course.

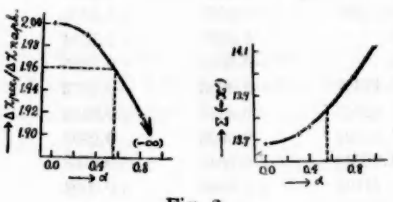

Fig. 2.

3. On the other hand, the increase of α reduces the diamagnetic anisotropy, and in the extreme case of $\alpha=0$, each $1\bar{1}$ or $1'\bar{1}$ being a pure single bond, the relative anisotropy is just equal to 2.0. This result is interesting; however, the alteration of the relative anisotropy with regard to α is very small except in the cases of $\alpha=0.9$ and 1.0 The experimental relative anisotropies in the preceding paper, being 1.96 and 2.02, lie within the range of $\alpha=0.0$ and 0.6.

In the special case of $\alpha=1$, as we see in Table 1, we have $x''=-\infty$ twice and $x''=0$ once, the latter representing a level which is not affected by the magnetic field. It is possible to consider that such unacceptable results may be ascribed to the quadruple roots of $x'=\pm1$, or to the highest symmetry of the model constructed with the same, five regular hexagons. As a matter of fact, it must be true that every carbon atom in aromatic rings, in general, cannot always be the same, except in the case of benzene. Therefore, there is a sufficient reason for omitting the case of $\alpha=1$ in this problem. Moreover, it must be borne in mind that the method of molecular orbitals neglects the r_{12} repulsion effects except in so far as it is represented by the Hartree's selfconsistent field, with the result that the multiple or ionic structure occurs with an excessive probability.[8] As the result of the same reason above, the $\Sigma(x')-\alpha$ curve in Fig. 2 is represented only by the attractive term wanting the repulsive one. In spite of such crudeness, the London theory is able to carry us to such a good agreement with experiment, so far from giving any discrepancy except the neighbors of $\alpha=1$.

On the other hand, however, according to Pauling's semi-classical theory, the diamagnetic anisotropy of perylene molecule has been shown to be about three times as large as that of naphthalene.[3] As pointed out by London [4], [5], the classical theory itself may be so far from giving any London (4), (5), the classical theory itself may be so far from giving any sufficient explanation about the diamagnetic anisotropy.

If we assume the model in Fig. 1 to be a peripheral form, in which we neglect the interactions between the π-electrons within the 10; 00'; 01'; $\bar{1}0$; $\bar{0}\bar{0}'$ and $\bar{0}\bar{1}'$ bonds, we can easily derive the general formula from

(8) cf. J. H. Van Vleck, and A. Sherman, *Rev. Mod. Phys.*, **7** (1935), 170.

the London theory as follows:

$$\Delta\chi_S/\Delta\chi_{\text{Benz.}} = (6\times n/N)^2 \times \sin\frac{\pi}{6} \Big/ \sin\frac{\pi}{N},$$

where

$$n = \frac{\text{the total area of the model in problem}}{\text{the area of benzene}},$$

and N is the number of π-electrons along the periphery. Putting $n=5$ and $N=18$, $\Delta\chi_{perv.}/\Delta\chi_B$ becomes 7.98, and in the case of $n=5$ and $N=20$, the corresponding value becomes 7.19. Both of them are far from being realized in experiment.

Summary

Applying London's theory of diamagnetic anisotropy, computations have been performed on the structure of perylene molecule. In this problem, the theory gives no definite value if we choose such a model constructed with the same, five regular hexagons as we usually do in the conventional method. Introducing a simple parameter, this difficulty is removed with the result that the relative diamagnetic anisotropy of this molecule is about twice as large as that of naphthalene, showing a good agreement with experiment. A model as a peripheral form gives a divergent result from experiment.

It is the pleasure of the present writer to express his sincere thanks to Professor H. Tominaga, Director of the Institute, for his kind interests and encouragements throughout the course of this study. He also thanks the Department of Education for the financial grant.

Glass Research Institute, Tohoku University, Sendai.

A New Method of the Colorimetric Determination of Small Amounts of Manganese with Silver Peroxide*

By Yukio MURAKAMI

(Received January 11, 1949)

Introduction. Small amounts of manganese can be determined accurately and quickly by the colorimetric method based upon the ease

* Presented before the Division of Inorganic and Analytical Chemistry at the Annual Meeting of the Chemical Society of Japan, Tokyo, April 2 to 4, 1948.

with which the manganese solution is oxidized to permanganate. Several oxidizing agents were proposed for this purpose by many workers. At first, lead peroxide was proposed for this purpose by Crum,[1] then sodium bismuthate was introduced by Reddrop and Ramage,[2] ammonium persulfate was tried in the presence of silver ion acting as catalyst by Marshall,[3] alkali periodate was recommended by Willard and Greathouse[4] and nickel dioxide was used by Lang.[5]

It is well known that the excess lead dioxide or sodium bismuthate is defective in that the excess of the reagent must be removed before the comparison can be made. In the application of persulfate, it is sometimes difficult to obtain correct results [4] [6], owing to the difficulty of complete oxidation. As some workers have recommended, the periodate method seems to be the best in overcoming these defects; however, it too has its handicap as it is exceedingly difficult to obtain a good quality and it is also too expensive for the routine work.[7]

In the persulfate method the amount of silver nitrate added is too large to consider its action simply as a catalyst. Therefore Barbier[8] has proposed such an intermediate compound as $3Ag_2O_2 \cdot AgNO_3$ for the process of oxidation, while on the other hand Pinkus[9] suggested the formation of silver peroxide. Although some investigators have studied this problem, none of them have been able to draw any definite conclusion.

The purpose of this investigation was therefore as follows: a) to isolate a silver compound with strong oxidizing power, b) to improve the colorimetric determination of manganese by the application of that compound.

Preparation of Silver Peroxide. On cautiously adding a slight excess of ammonium persulfate to a 10 per cent solution of silver nitrate, stirring constantly, a heavy gray precipitate is soon separated and the supernatant liquid is tinted brown. This gray precipitate is considered to be a mixture of silver peroxide and silver persulfate and the brown liquid is a nitric acid solution of silver peroxide from which silver peroxide can be precipitated when it is diluted. It is washed several times by decantation and transfered to an amber glass stoppered bottle with some water. It is desirable that this be kept in a dark cold place.

(1) W. Crum, *Lieb. Ann.*, **55** (1845), 219; R. Wasmuth, *Ang. Chem.*, **42** (1929), 133.

(2) J. Reddrop and H. Ramage, *Trans. Chem. Soc.*, **67** (1895), 268; R. O. Gortner and C. O. Rost, *Ind. Eng. Chem.*, **4** (1912), 522.

(3) H. Marshall, *Chem. News*, **83** (1901), 76; M. Dittrich, *Z. anorg. allgem. Chem.*, **80** (1913), 171; R. Lang and F. Kurtz, *Z. Anal. Chem.*, **85** (1931), 181.

(4) H. H. Willard, and L. H. Greathouse, *J. Am. Chem. Soc.*, **39** (1917), 2366.

(5) R. Lang, *Z. anorg. Chem.*, **158** (1926), 370.

(6) R. O. Gortner and C. O. Rost, *Ind. Eng. Chem.*, **4** (1912), 522.

(7) H. H. Willard and J. J. Thompson, *Ind. Eng. Chem., Anal. Ed.*, **3** (1931), 399; G. J. Hough, *Ind. Eng. Chem., Anal. Ed.*, **7** (1935), 408.

(8) G. A. Barbier, *Ber.*, **60** (1927), 2424; A. Travers, *Compt. rend.*, **182** (1926), 972.

(9) A. Pinkus and L. Ramakers, *Chem. Zentr.*, **1** (1933), 1658; *Bull. Soc. Chem., Belgium*, **41** (1933), 529.

The precipitate thus obtained will be employed as a new energetic oxidizing agent and, for the sake of convenience, is called silver peroxide hereafter though it may be a mixture as mentioned above. A freshly precipitated silver peroxide may on standing undergo a change in contact with water forming a darker precipitate. It is supposed that the following reaction takes place[10]: $Ag_2S_2O_8+2H_2O \rightarrow Ag_2O_2+2H_2SO_4$

When silver peroxide is added to the solution containing manganese acidified with sulfuric acid it is decomposed in a little while in the following way: $Ag_2O_2+H_2SO_4 \rightarrow Ag_2SO_4+H_2O+O$

In this case the silver sulfate thus formed is a strong catalyst which decomposes hydrogen peroxide and liberates oxygen in the nascent state in the acid solution.

The oxidizing power of silver peroxide is retained for approximately half a year or more without any decrease in power as shown in Table 1.

Table 1. Oxidizing power and the duration after preparation.

Duration after preparation (days)	1	7	14	21	28	67	148
MnO found (γ)	104.1	104.2	*104.0	104.1	104.1	103.9	104.2

The tested solution contains 140.0 γ MnO in 25 c.c. solution acidified with sulfuric acid.

Outline of Method.

A stock solution of manganese sulfate containing 0.1g. of MnO per liter is prepared by reducing potassium permanganate solution in the usual way. The standard solution of manganese containing 104.0 γ of MnO used in this investigation was obtained by suitably diluting the above stock solution.

The addition of silver peroxide (name given the precipitate as aforementioned) to the acidified solution containing manganese, at room temperature and with stirring, instantaneously produces the maximum coloration due to the formation of permanganate ion. Any excess of the reagent which is left suspending in the solution is easily decomposed by warming on a water bath for 2 to 3 minutes after which the solution will be left clear. The relation between the time and temperature required for the decomposition is shown in Table 2. Though the duration after the reagent has been prepared does not reduce its oxidizing power it has been found that decomposition of excess reagent becomes quicker by long standing.

Table 2. Time required for complete decomposition at various temperatures.

°C / days	92.5	70	60	50	40	20	10
2	3 min.	9 min.	13 min.	24 min.	45 min.	— min.	— min.
13	2	—	3	—	6	10	—
21	2	—	2	—	3	—	8

(10) Mellor, "Comprehensive Treatise on Inorganic and Theoretical Chemistry," vol. III. p. 383, New York (1929): W. Machu, "Das Wasserstoff Peroxide und die Perverbindungen," S. 236, Wien (1937),

Through this experiment the Pulfrich photometer with filter S53 (maximum absorption 530 mμ) was used. As previous workers have reported, it was found that the Lambert-Beer's law holds closely in this method.

(a) **Concentration of sulfuric acid.** The oxidation is carried out at various concentrations as shown in Table 3. Best results were obtained by using 8 to 12 per cent sulfuric acid solution. In the following experiments, a 10 per cent solution was used with a few exceptions.

Table 3. Suitable concentration of sulfuric acid.

Concentration of H_2SO_4 (%)	MnO found (γ)		% of coloration*	
1	82.7	84.0	79.5	80.7
5	98.2	96.7	94.4	93.0
8	104.0	103.4	100.0	99.4
12	103.7	104.3	99.7	100.3
25	103.4	103.1	99.4	99.2
30	97.8	96.3	94.0	92.8

* % of coloration is calculated from MnO (found)/MnO (calculated). In the above MnO (calculated) is 104.0 γ.

(b) **Quantity of oxidizing agent.** It is convenient to handle about 0.1 to 0.15 g. (call this one unit). About 100 γ MnO is oxidized sufficiently by one unit as shown in Table 4. Only two units of silver peroxide is sufficient to oxidize about 800 γ manganese as MnO. If the MnO concentration is more than 10 p. p. m., the violet precipitate, presumably siver permanganate, is formed. It is, therefore, preferable to use the sample solution containing less than 10 p. p. m. of manganese as MnO.

Table 4. Amounts of silver peroxide necessary for oxidation of manganese.

Quantity (unit)	1/2		1		15		15	
MnO found (γ)	90.5	93.4	104.3	103.7	104.3	104.1	104.0	104.3
Difference (γ)	−13.5	−10.6	+0.3	−0.3	+0.3	+0.1	0	+0.3

The test solution contains 104.0 γ manganese as MnO in 25 c.c.

(c) **Removal of excess silver peroxide.** The addition of the reagent darkens the solution. However this excess can be removed only by warming it on a water bath or by letting the solution stand for several minutes as described already. The reagent should not in any case be added to a hot solution as oxidation will no doubt be insufficient. Maximum coloration is obtained by a 2 minutes heating. Undue prolonged heating reduces the coloration.

Table 5. Differences due to heating time.

Heating time (min.)	2	4	5	7	10
MnO found (γ)	104.0	103.6	102.5	97.0	77.3
Difference (γ)	0	−0.4	−1.5	−7.0	−26.7

The test solution contains 104.0 γ manganese as MnO in 25 c.c.

(d) Standard curve and accuracy. Oxidation of the various concentrations of manganese is performed in strict adherence to the condition as already established. The extinction coefficient of permanganate solution thus obtained was measured with the results shown in Table 6.

Table 6. Extinction coefficients of the solutions after oxidation of manganese by silver peroxide.

Manganese as MnO in p. p. m.	2.80	4.16	6.24	8.32
No. 1 (av. of eight readings)	0.2002	0.4039	0.6043	0.8048
No. 2 (av. of eight readings)	0.2009	0.4028	0.6034	0.8057
No. 3 (av. of eight readings)	0.2008	0.4013	0.6052	0.8059
No. 4 (av. of eight readings)	0.2018	0.4041	0.6044	0.8049
No. 5 (av. of eight readings)	0.2022	0.4017	0.6043	0.8056
Average	0.2012	0.4028	0.6037	0.8052

Filter: S53, length of the cell: 30.04 mm.

From these data the following relation between concentration and extinction coefficient is calculated by the application of least squares where X is the concentration of manganese as MnO in p. p. m. and E, the ex inction coefficient of the length of 10.00 mm. cell used.

$$X = 3.439\ E$$

To make sure of this relation, the extinction coefficient of permanganate solution having the same acidity was measured at various concentrations as shown in Table 7 (A). The same relation was obtained.

$$X = 3.435\ E$$

It was found that results obtained by this proposed method coincide with the true value allowing for minimum difference. In other words, the accuracy of this method is proved to be satisfactory.

For purpose of comparison the potassium permanganate is treated in the same way as mentioned above (see Table 7 (B)). The following equation was obtained in the same way from the results which were cited in Table 7 (B).

$$X = 3.439\ E$$

Table 7. Extinction coefficients of potassium permanganate solution when oxidation is done (B) or not (A).

E / MnO Exp. p. p. m.	A				B			
	No. 1	No. 2	No. 3	Ave.	No. 1	No. 2	No. 3	Ave.
1.992	0.1938	0.1935	0.1922	0.1932	0.1929	0.1931	0.1918	0.1926
3.984	0.3868	0.3860	0.3851	0.3859	0.3864	0.3859	0.3852	0.3858
5.976	0.5799	0.5780	0.5807	0.5795	0.5787	0.5793	0.5779	0.5786
7.968	0.7733	0.7720	0.7716	0.7723	0.7728	0.7710	0.7714	0.7717

E: Average of eight readings in one determination. Filter: S53, the length of the cell: 30.04 mm.

The results obtained correspond with the true value thus proving that silver peroxide has no obstructive effects on the process of oxidation. Thus it can be concluded from these results that silver peroxide is a superior oxidizing agent.

(e) **Reproducibility.** The following experiments were carried out to certify the accuracy of this method at various concentrations of manganese.

Table 8. Reproducibility of this method.

MnO present	MnO found (γ)					E	
						min.	max.
104.0 γ in 50 c.c.	103.4	103.8	103.7	104.3	104.5	0.2002	0.2022
104.0 γ in 25 c.c.	104.3	104.0	103.7	104.4	103.7	0.4013	0.4041
208.0 γ in 25 c.c.	207.9	208.1	208.2	207.9	208.1	0.8048	0.8059
312.0 γ in 50 c.c.	312.2	311.8	312.7	312.3	312.2	0.6034	0.6052
832.0 γ in 200 c.c.	828.5	830.4	829.5	832.2	831.0	0.4009	0.4027

E: Average of eight readings in one determination. Silver oxide: 2 units, acid concentration: 8%. Filter: S53, the length of the cell: 30.04 mm.

Thus it was proved that the proposed method may be used satisfactorily as a quick and accurate colorimetric method. Whatever difference may be caused it will be limited to 1.5 per cent.

(f) **Interference of various ions.** It is necessary to study the interference of various ions as the oxidizing agent used herr has been newly tried.

The interference ions are divided into three groups: 1) colorless ions, 2) colored ions, 3) ions precipitated by silver, sulfate ions or in acid solution.

(1) Colorless ions. Some colorless ions do not interfere with the colorimetric determination of manganese as would be expected. As a large quantity of ferric ion interferes with the coloration of the permanganate, the addition of phosphoric acid is necessary to prevent this interference. Some reducing ions, namely ferrous, sulfite, nitrite, oxalate, tartrate and other oxidizable organic anions in small amounts can be easily oxidized with further addition of silver peroxide. White silver sulfate will sometimes precipitate. In this case it is desirable to reoxidize after filtering off. If a large amount of such ions is present, it is safer to remove or destroy the ions by evaporation with nitric acid or a mixture of nitric acid and sulfuric acid before the oxidation is carried out. (see Table 9).

(2) Colored ions. Some interferences are expected when the colored ions are present in the sample solution. However the effect of some of these may be compensated by the use of an aliquot portion or by the addition of the same amount in the reference cell of photometer as shown in Table 10.

As the above tests have indicated there is no obstacle met by the presence of these ions especially chromium, titanium, up to the above concentration in the application of this new reagent. None of these interferences need be considered because the cited ions can be easily separated by the usual method.

(3) Ions precipitated by silver ion, sulfate ion or in acid solution. Chloride precipitates by a slight excess of silver nitrate. However it is preferable to remove it by evaporation with sulfuric acid. Other ions may be removed simply by filtration with no serious effects as shown in Table 11.

Proposed Method. As already described it is proved that the colorimetric determination of manganese may be successfully performed by utilizing the new oxidizing agent. The general procedure will be des-

Table 9. Ions which have no interfering effect.

Ions	Salt used	Amount present (against 104.0 γ MnO) (mg.)		MnO found (γ)	Difference (γ)
Al^{+++}	$Al_2(SO_4)_3$	Al	100 (1:1000)	103.8	−0.2
As^{+++}	As_2O_3	As_2O_3	100 (1:100)	103.8	−0.2
NH_4^+	$(NH_4)_2SO_4$	NH_4	100 (1:1000)	103.8	−0.2
Bi^{+++}	$Bi(NO_3)_3$	Bi	10 (1:100)	104.0	0
Ca^{++}	$Ca(NO_3)_2$	Ca	10 (1:100)	104.0	0
Cd^{++}	$Cd(NO_3)_2$	Cd	100 (1:1000)	103.6	−0.4
Fe^{+++}	$Fe(NO_3)_3$	Fe	100 (1:1000)	104.0	0
Mg^{++}	$MgSO_4$	Mg	100 (1:1000)	103.4	−0.6
Sn^{++++}	$Sn(SO_4)_2$	Sn	100 (1:1000)	103.9	−0.1
Tl^+	Tl_2SO_4	Tl	10 (1:100)	103.3	−0.7
Zn^{++}	$ZnSO_4$	Zn	100 (1:1000)	103.6	−0.4
VO_3^-	NH_4VO_3	V_2O_5	10 (1:100)	104.2	+0.2
BO_2^-	$Na_2B_4O_7$	B_2O_3	100 (1:1000)	103.7	−0.3
MoO_4^{--}	$(NH_4)_6Mo_7O_{24}4H_2O$	MoO_3	140 (1:1400)	104.2	+0.2
PO_4^{---}	Na_2HPO_4	P_2O_5	1000 (1:10000)	104.0	0
SiO_3^{--}	Na_2SiO_3	SiO_2	5 (1:50)	104.1	+0.1
F^-	NaF	F	0.16 (1:1.6)	104.0	0
NO_3^-	HNO_3	NO_3	2.8 (1:28000)	104.0	0
PO_4^{---}	H_3PO_4	P_2O_5	1500 (1:15000)	104.4	+0.4
$C_2O_4^{--}$	$(COONa)_2$	C_2O_4	14 (1:140)	104.2	+0.2
$C_4H_4O_6^{--}$	$NaKC_4H_4O_6$	$C_4H_4O_6$	5 (1:50)	103.8	−0.2

Table 10. Colored ions.

Ions	Salt used	Amount present (against 104.0γ) (mg.)		MnO found (γ)	Difference. (γ)	Remarks
Cr^{+++}	Chrom-alum	Cr 10	(1:100)	103.2	−0.8	after oxidation with Na_2O_2
$Cr_2O_7^{--}$	K_2CrO_4	Cr 10	(1:100)	104.1	+0.1	
Cu^{++}	$CuSO_4$	Cu 100	(1:1000)	104.2	+0.2	
Cu^{++}	$CuSO_4$	Cu 100	(1:1000)	104.3	+0.3	isolated as CuS
Nd^{+++}	$Nd(NO_3)_3$	Nd_2O_3 50	(1:500)	104.6	+0.6	
Ni^{++}	$NiSO_4$	Ni 50	(1:500)	104.5	+0.5	acid concentration 25%
Ti^{++++}	$Ti(OH)_4$	TiO_2 10	(1:100)	104.0	0	added 10 units
rare earths	nitrate	about 50	(1:500)	103.8	−0.2	$Nd(NO_3)_3$ containing other rare earths
Co^{++}	$CoSO_4$	Co 10	(1:100)	104.3	+0.3	the comparison solution must be treated as a sample with silver peroxide

cribed below. If the sample contains a large amount of chloride add sulfuric acid and evaporate until fumes of the latter appear. If the amount of chloride is small it may be separated as silver chloride.

Table 11. Ions precipitated in the procedure.

Ions	Salt used	Amount present against 104.0 γ (mg.)		MnO found (γ)	Difference (γ)	Remarks
Ba^{++}	$Ba(NO_3)_2$	Ba	100 (1:1000)	104.6	+0.6	
Sr^{++}	$Sr(NO_3)_2$	Sr	100 (1:1000)	104.0	0	
Hg_2^{++}	$Hg_2(NO_3)_2$	Hg	100 (1:1000)	103.8	−0.2	
Cl^-	NaCl	Cl	100 (1:1000)	103.8	−0.2	
Pb^{++}	$Pb(NO_3)_2$	Pb	100 (1:1000)	104.0	0	
Ca^{++}	$Ca(NO_3)_2$	Ca	100 (1:1000)	103.7	−0.3	alcohol added to decrease the solubility
Ca^{++}	$Ca(NO_3)_2$	Ca	50 (1:500)	104.1	+0.1	isolated as oxalate
SiO_3^{--}	Na_2SiO_3	SiO_2	100 (1:1000)	103.8	−0.2	separated as insoluble SiO_2
SiO_3^{--}	Na_2SiO_3	SiO_2	100 (1:1000)	104.3	+0.3	SiO_2 filtered off after treating with H_2SO_4.
WO_4^{--}	Na_2WO_4	W	100 (1:1000)	104.1	+0.1	digested with HNO_3 and filtered

In the presence of a large quantity of ferrous ion and other oxidizable substance, boil with nitric acid or add the later before evaporating with sulfuric acid. The best method for the separation of chromium involves oxidation in basic solution as many workers have recommended, whereby manganese is precipitated with iron, titanium and others. In like manner other undesirable matter can be easily separated from manganese with no interfering effects.

It is most convenient to apply hydroxide precipitation method with a little ferric salt as a collector to concentrate very small amounts of manganese as in the case of natural water (as little as 10 γ per liter). The sample solution thus obtained ready for colorimetric determination should contain 10 per cent of sulfuric acid in the final step. Then add about 0.1 g. silver peroxide stirring constantly. Heat on water bath for 2 minutes or let stand for several minutes to obtain the maximum coloration of the manganese. Dilute to the definite volume and make the color comparison in any convenient way.

By this method as little as 1 p.p.m. of manganese (as MnO) can be easily determined with the best results. This method was retested by determining manganese in natural water, hot springs water and biological materials, results of which will be given in a latter communication.

Summary

In face of several defects noted by the oxidation agents hitherto used in the determination of manganese by the colorimetric method a new reagent, so-called "Silver peroxide," has been proposed. This new reagent

has been found to excel other reagents in the following respects: a) easy preparation and easy decomposition of the excess reagent, b) strong oxidizing power not reduced by long standing and cheap availability for routine work, c) no noticeable interference by other reagents during action and accuracy in results obtained.

Thus by its use the procedure is exceedingly simplified and the time required is considerably less than that in the method used hitherto.

The author wishes to express his sincere appreciation to Professor Kenjiro Kimura for his valuable suggestion and his never-failing encouragement during this investigation. He is also grateful to Mr. M. Tanaka for his helpful advice and sincere friendship which facilitated this work.

Chemical Institute, Faculty of Science,
Tokyo University.

The Theory of the Rubber-like Elasticity in Monolayers.[1]

By Keizō SUZUKI.

(Received February 1, 1949.)

Introduction. When a monolayer is made from high-molecular compound with rubber-like elasticity, what are its properties?

We succeeded in making a monolayer by dropping the benzene solution of the addition polymer of butadiene with acrylonitrile onto the water surface, and measured the surface pressure changing the surface area and temperature[2] (Fig. 1). The monolayer takes the most extended form under no external force. On the contrary the three-dimensional rubber block set free assumes the most contracted form as well known. A thin rubber layer on water which has a similar nature to the three-dimensional one was studied by Trapeznikov,[3] but it is too thick to be called a monolayer.

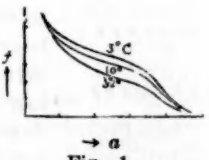

Fig. 1.

Fig. 1. The surface pressure and the surface area of the monolayer of addition polymer from butadiene 5 and acrylonitrile 2.

This difference between the two states of the substances seems, at first sight, to be a serious hindrance for us to find common properties in them. But we find the expression of the rubber-like elasticity in the two

(1) Short abstract of the mathematical part is already reported in Japanese. K. Suzuki and Y. Suzuki, *Kagaku*, **17** (1947), 238.
(2) K. Suzuki, *J. Chem. Soc. Japan*, **63** (1942), 1058.
(3) A. A. Trapeznikov, *Compt. rend. U. R. S. S.*, **95** (1941), 138.

properties of the monolayer: extraordinarily large and reversible compressibility over a wide range of the area, and the decrease of the surface area and surface pressure with increasing temperature.

The Structure of the Monolayer. Can all the substances with rubber-like elasticity spread to monolayers? No; for example, natural cauchouc can never spread to the monolayer on water, for it has no "hydrophilic groups". The monolayer on water, generally speaking, can be formed only by the partially hydrophobic and partially hydrophilic molecules.[4] High polymeric molecules with hydrophobic backbones must have hydrophilic radicals to spread to monolayers; our sample has the nitrile groups. Another sample with phenyl radicals instead of nitriles failed to spread.

The hydrophilic radicals, which take the states of lower energy by attaching to water, tend to spread the molecule broader and thinner on the water surface, and on the other hand the thermal motion of the molecular chains tends to contract to the more coiled and gathered forms, the more probable state, like the three-dimensional case. The balance of the two forces appears to us as the properties of the monolayer above shown. The elevation of temperature increases the thermal motion and contracts the area of the film.

As long as we call the spontaneous contraction of the long chain molecule by thermal motion as the rubber-like elasticity,[5] we must regard the nature of this monolayer as an expression of the same sort of elasticity. The statistical treatment on the elasticity has had successful results. We shall now try a statistical evaluation of the mechanical and thermodynamical properties of the monolayer.

Fig. 2.

Fig. 2. The schema compression.

We must set up a model which fits this monolayer. The observed nature does not permit the simple translation of the finely constructed three-dimensinoal theory to the two-dimensional one. Our model must be able to bear under the reversible compression to the fairly thick layer which may irreversibly destroy the monolayers of low molecular compounds. By this compression some parts our molecule are pushed up from the water surface but they are ready to return to the water surface by the release from the compression (Fig. 2). This is the reason why the two-dimensional model cannot be adopted for our monolayer, although it was recently applied for some polymeric monolayer of the expanded type by Singer.[6]

Probability for Configurations of the Chain. We consider a long chain molecule with n hydrophilic groups in equal intervals. Let the intervals be m-membered chains, then the molecule is mn-membered

(4) N. K. Adam, "The Physics and Chemistry of Surfaces," (Oxford 1941), Chapt. II.
(5) W. Kuhn, *Kolloid-Z.*, **86** (1936), 258; H. Dostal, *Mh. Chem.*, **71** (1938), 144; F. Horst Müller. *Kolloid-Z.*, **95** (1941), 138; R. Kubo, *Proc. Phys. Soc. Japan*, **2** (1947), 51.
(6) S. J. Singer, *J. Chem. Phys.*, **16** (1948), 842.

$(n \gg 1)$ (Fig. 3).

We shall estimate the probability $W_{\alpha n}$ that αn hydrophilic groups are in contact with water surface and $(1-\alpha)\ n$ groups are not. For a while we put the energy difference due to the hydration out of consideration. Let u_i be the probability that when a certain group is on water the i-th group from it is on water and the intervening i-1 groups are not.

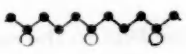

Fig. 3.

Fig. 3. The linear molecule.

Then the probability that the chain takes the configuration in Fig. 4 is $u_3u_2u_1u_1$. Generally it becomes the product of $\alpha n u_i s$, where the sum of is becomes n. The number of selection of αn groups is ${}_nC_{\alpha n}$, then the probability $W_{\alpha n}$ is the sum of ${}_nC_{\alpha n}$ products similar to the product above shown:

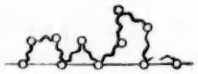

Fig. 4.

Fig. 4. A schematic configuration.

$$W_{\alpha n} = \sum^{{}_nC_{\alpha n}} \prod^{\alpha n} u_i. \qquad (1)$$

This is obtained as the factor of x^n of $(\sum_i u_i x^i)^{\alpha n}$:

$$\sum_n W_{\alpha n} x^n = (\sum_i u_i x^i)^{\alpha n}. \qquad (2)$$

Next we rewrite u_i in the calculable form. Let p_i be the probability that when a certain group is on water the i-th group from it is on water too. p_i contains, contrary to u_i the cases that some of the i-1 intervening groups are on water. p_0 is the probability that when a group is on water the same group is on water, therefore

$$p_0 = 1.$$

p_1 is the probability that the next group is on water. In this case there is no intervening group, therefore

$$p_1 = u_1.$$

p_2 is the probability that the second group is on water, and is the sum of two cases: the case where the intervening group is on water and the case that it is not. The probabilities are

$$u_1u_1 \text{ or } u_1p_1,\ u_2 \text{ or } u_2p_0$$

respectively. And then we have

$$p_2 = u_1p_1 + u_2p_0.$$

Similarly p_3 is separated into three cases and

$$p_3 = u_1p_2 + u_2p_1 + u_3p_0$$

is obtained. Generally p_j is separated into j terms: the first group is on

water $= u_1 p_{j-1}$, the second group is on water $= u_2 p_{j-2}$, and the i-th group is on water $= u_i p_{j-i}$. Then

$$p_j = \sum_{i=1}^{j} u_i p_{j-i} . \tag{3}$$

These lead to the equation:

$$p_1 x + p_2 x^2 + \ldots = (p_0 + p_1 x + \ldots)(u_1 x + u_2 x^2 + \ldots),$$

which gives the mother function of u_i by a transformation:

$$\sum_{i=1}^{\infty} u_i x^i = \sum_{i=1}^{\infty} p_i x^i \Big/ \sum_{i=0}^{\infty} p_i x^i . \tag{4}$$

Putting this in (2), we have

$$\sum_{n} W_{\alpha n} x^n = \Big(\sum_{i=1}^{\infty} p_i x^i \Big/ \sum_{i=0}^{\infty} p_i x^i\Big)^{\alpha n} \tag{5}$$

We shall now consider how p_is be expressed. p_i is the probability that when an end of the im-membered chain is on water another end is also on water.

The Brownian movement gives a good analogy. Let us estimate the probability that a particle which started from a planar wall at time 0 comes back to and collides with the wall at time im. Let the wall be the plane $z=0$. We compare two sorts of traces of the particle which was on $z=0$ at $t=0$: one where the wall is perfectly elastic and the other where there is no wall. The traces of the former are obtained from those of the latter by folding the one half on the side of the negative z on to the other half (Fig. 5).

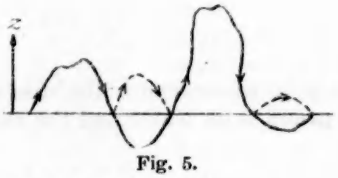

Fig. 5.

Fig. 5. A trace of a Brownian particle about an elastic wall.

Therefore the probability that the particle of the first kind passes through the plane $z=0$ in the time interval $t \sim t+dt$ equals the probability that the particle of the second collides in the same time.

Similarly p_i is otained as the probability that when an end of the im-membered chain is on the plane $z=0$ another end is also on the plane. Here the plane is not a wall nor a water surface but an imagined geometrical surface.

Thus p_i can be known from the degree of flexibility of the chain. The more flexible the chain, the larger becomes p_i.

The estimation of p_i is perfectly mathematical on the simple chain, each unit of which has equal probability, 1/2, to take +1 or −1 as the z-component of its length:

$$p_0 = 1,\ p_1 = {}_mC_{m/2}\,2^{-m},\ p_2 = {}_{2m}C_m 2^{-2m},$$
$$p_i = {}_{im}C_{im/2}\,2^{-im} \simeq (\pi m/2)^{-0.5}\, i^{-0.5}.$$

If im is not so small, p_i is generally approximated as

$$p_0 = 1,\ p_i = Bi^{-0.5} \text{ for } i > 1, \qquad (6)$$

where B is a constant proportional to the reciprocal square root of m, for the distribution of the relative position of the two ends of a chain is well approximated by the Gaussian distribution.[1],[7]

Putting i=1 in (6), we have B=p_1. B is the probability that when one end of m-membered chain is on water the other is also on it. This probability must be proportional to the square root of m, and the proportional constant can be known from the nature of the chain, from the pseudosegment[8] expressing the flexibility and the width of the potential valley at the surface of water for the hydrophilic group. A further estimation is deferred to another paper and here only the qualitative conclusion is stated: the more flexible chains with hydrophilic radicals in shorter intervals have larger values of B.

Surface Pressure. Statistical thermodynamics tells us the equation

$$fnda = -kTd \log Z_{an}, \qquad (7)$$

where f is the surface pressure, a is the surface area per radical, and Z_{an} is the partition function. $fnda$ is the work done by the molecule with the increase of area nda, so it is equal to the decrease of the free energy $-kTd \log Z_{an}$.

We have neglected the energy due to the hydration of hydrophilic groups in the calculation of W_{an}. Therefore the partition function is substituted by W_{an} multiplied by exp $(-\varepsilon an/kT)$, in which ε is the hydration energy of a group k is the Boltzmann's constant, and T is absolute temperature. Then the equation (7) gives

$$f = \left(\varepsilon + \frac{kT}{n}\frac{d}{da}\log W_{an}\right)\frac{da}{da}. \qquad (8)$$

The differential calculus in the bracket is carried by the use of the mother function of W_{an} (5):

$$W_{an} = \frac{1}{2\pi\lambda}\oint \frac{dx}{x^{n+1}}\left(\sum_{i=1}^{\infty} p_i x^i \Big/ \sum_{i=0}^{\infty} p_i x^i\right)^{an},$$

where λ is $\sqrt{-1}$, i in the ordinary notation. Approximation at the saddle point leads to

(7) S. Chandrasekhar, *Rev. Mod. Phys.*, **15** (1943), 3~16.
(8) K. Suzuki, this Bulletin, **20** (1947), 19.

$$W_{an} = x^{-n}\left(\sum_{i=1}^{\infty} p_i x^i \Big/ \sum_{i=0}^{\infty} p_i x^i\right)^{an} \cdots\cdots,$$

$$\frac{d}{da}\log W_{an} = n\log\left(\sum_{i=1}^{\infty} p_i x^i \Big/ \sum_{i=0}^{\infty} p_i x^i\right), \qquad (9)$$

in which x is the value corresponding to the extreme value of the integrand in the course of the integration. x is given by the equation

$$a = \sum_{i=1}^{\infty} p_i x^i \sum_{i=0}^{\infty} p_i x^i \Big/ \sum_{i=1}^{\infty} i p_i x^i, \qquad (10)$$

which is obtained by equating the differential coefficient of the logarithm of the integrand to zero. Inserting (9) in (8) one obtains

$$f = \left\{\varepsilon + kT\log\left(\sum_{i=1}^{\infty} p_i x^i \Big/ \sum_{i=0}^{\infty} p_i x^i\right)\right\} da/da, \qquad (11)$$

in which x is given by (10). The use of (6) for p_i in (10) and (11) yields

$$f = \left[\varepsilon - kT\log\left\{\left(B\sum_{i=1}^{\infty} i^{-0.5} x^i\right)^{-1} + 1\right\}\right] da/da, \qquad (12)^{(9)}$$

$$a = \sum_{i=1}^{\infty} i^{-0.5} x^i \left(1 + B\sum_{i=1}^{\infty} i^{-0.5} x^i\right) \Big/ \sum_{i=1}^{\infty} i^{0.5} x^i. \qquad (13)^{(9)}$$

Surface pressure is independent of molecular weight or polymerization degree n, but depends only on the hydrophilicity ε of the groups and

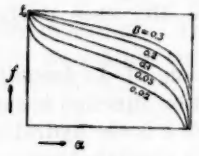

Fig. 6.

Fig. 6. Calculated Relations of f with a.

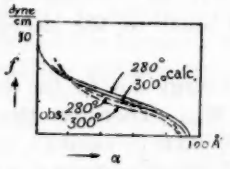

Fig. 7.

Fig. 7. Comparison of theory and observation. Calc.: $B = 0.02$, $da/d\alpha = 100$ Å^2, $\varepsilon = 3.10^{-13}$ erg. Obs.: polymer from butadiene 5 and acrylonitrile 1.

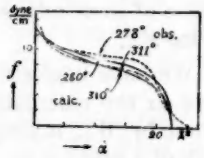

Fig. 8.

Fig. 8. Comparison of theory and observation. Calc.: $B = 0.1$, $da/d\alpha = 23$ Å^2, $\varepsilon = 1.3\cdot10^{-13}$ erg. Obs.: polymethylsiloxane.

the flexibility B of the m-membered chain.

The Numerical Results. Calculated relations of f with a are

(9) The numerical summations of the series in (12) and (13) are carried by the equations:

$$\sum i^{0.5} x^i = \frac{\sqrt{\pi}}{2}\{(1-x)^{-1.5} - x\} + \sum\left(i^{0.5} - \frac{\sqrt{\pi}}{2}\cdot\frac{3}{2}\cdot\frac{5}{4}\cdots\frac{2i-1}{2i-2}\right)x^i,$$

$$\sum i^{-0.5} x^i = \sqrt{\pi}\{(1-x)^{-0.5} - 1\} + \sum\left(i^{-0.5} - \frac{\sqrt{\pi}}{2}\cdot\frac{3}{4}\cdot\frac{5}{6}\cdots\frac{2i-1}{2i}\right)x^i.$$

plotted in Fig. 6 assuming the constant ε, T, and da/da. If the energy s becomes large f_0 becomes large and the curves move upwards conserving the forms. If the temperature becomes high, f_0-f becomes large proportionally to T. ($f_0=\varepsilon da/da$).

Experimental curves are compared with the theoretical ones in Fig. 7. The monolayer of polymethylsiloxane in Fig. 8 studied by Fox, Taylor, and Zisman[10] fits the larger B, for the molecule has more consecutive hydrophilic parts. They assume a particular structure, the helic form of the chain, but such a somewhat regular structure may not explain the temperature effect. It is necessary that the compression increases the entropy. The constant surface potential over the wide range of compression observed by Fox *et.al.* shows the validity of the assumption of constant da/da; because the constant da/da means the constant number of oriented radicals per area, and only the oriented ones are effective to surface potential, for the moments of the others take random directions and cancel each other.

Conclusion. It is a destined difficulty in the problem of the rubber elasticity what kind of macroscopic variable is combined with the microscopic thermal motion, since Kuhn assumed that the relative movement of the two ends of the chain is proportional to the macroscopic transformation.

In this theory the surface area is reasonably combined with the number of hydrated hydrophilic groups.

The second difficulty is the interaction of molecules, which is usually neglected and in this theory too. But we may expect the effect of the negligence to be smaller in the monolayer, because the chains are set more free from each other in it than in the three-dimensionally filled cases.

Thus the theory of the statistical elasticity seems to find the first step for its quantitative explanation.

Summary.

A discussion is made on the structure of the monolayer of the rubber-like highpolymer, and the equation of state is derived from the statistical theory. The extraordinarily large compressibility and the inverse temperature effect observed in the experiment are explained to be the expressions of the rubber-like elasticity. The theory is not a simple translation of the 3-dimensional theory to the 2-dimensional one.

The author wishes to express his sincere thanks to Yasutaka Suzuki for his remarkable contribution on the mathematical parts of this work.

Masaoka-cho, Toyokawa, Aichi pref.,
Japan.

(10) H. W. Fox, P. W. Taylor, and W. A. Zisman, *Ind. Eng. Chem.*, **39** (1947), 1401. They also found the gradual metamorphosis of the rubber monolayer into the expanded film, which we reported in (2).

Über den Reaktionsmechanismus der Dianthracenbildung aus Anthracen. II.

Von Momotaro SUZUKI.

(Eingegangen am 1. Februar 1949.)

In einer früheren Mitteilung[1] haben wir die folgenden Ergebnisse über die Photopolymerisation des Anthracens ins Dianthracen berichtet.

1. Bei kleinerer Anfangskonzentration des Anthracens nimmt die Menge des gebildeten Dianthracens mit der Konzentration zu. Wir wollen dieses Konzentrationsgebiet hier Gebiet A nennen.

2. Oberhalb eines bestimmten A_0 der Anthracenkonzentration ist die Menge des gebildeten Dianthracens unabhängig von der Konzentration des Anthracens. Dieses Gebiet nennen Wir Gebiet B und in der früheren Arbeit hat es sich hauptsächlich um den Reaktionsmechanismus in diesem Gebiet gehandelt. Ein Mechanismuschema ist vorgeschlagen, womit erklärt werden soll, dass diese Umsetzung trotz bimolekularer Bildungsweise eine Art von nullter Ordnung aufweist. Man hat übrigens die gute Übereinstimmung der Versuchsergebnisse mit der angenonmenen Postulation festgestellt.

In dem vorliegenden Teil sollen dieselben durch einige Versuche ergänzt werden, welche zu bestimmen, später näher zu diskutierenden Zwecken ausgeführt wurden. Alsdann haben wir den Messbereich der Konzentrationen des Anthracens sowie die Versuchstemperaturen noch weiter variiert, den experimentellen Befund zu prüfen und zu untersuchen, ob er sich mit dem vorgeschlagenen Reaktionsschema und den davon abhängenden Postulationen erklären lässt.

Versuchsanordnung und Durchführung. Die Versuchsanordnung und Durchführung der Versuche waren die gleiche, wie wir sie bereits in der vorigen Mitteilung beschrieben haben. Es kann wegen aller Einzelheiten derselben auf die dort gegebene Beschreibung verwiesen werden. Nur einige Kleinigkeiten waren geändert; und zwar die Umgebungstemperatur der Quecksilberbogenlampe, die als Lichtquelle diente, konstant zu erhalten, um die Lichtintensität des ins Reaktionsgefäss einfallenden Lichtes noch genauer konstant erhalten zu können.

Die Anfangskonzentration des Anthracens wurde noch weiter verändert und die Messung bei drei Temperaturen, d.i. -10°, 0° und 30° durchgeführt.

Die Reinigung der Materialien geschah auch in genau gleicher weise wie beim vorigen Versuch.

Messresultate. In der Tabelle 1, sowie auch in Fig. 1 sind die Versuchsergebnisse aufgezeichnet. Bei den Kurven in der Figur ist die in einer bestimmten Belichtungszeit, und zwar in 7.0 sowie auch 5.0 Stunden

(1) M. Suzuki, I. Mitteilung, dies Bulletin, **18** (1943), 146.

gebildete Menge des Dianthracens bei verschiedener Reaktionstemperatur gegen die Anfangskonzentration des Anthracens aufgetragen. Die linken Teile der Kurven zeigen genau dieselben Verläufe wie in Fig. 5 der vorigen Mitteilung. Wir sehen aber beim höheren Konzentrationsgebiet, dass noch eine andere Art Reaktionsverlauf vorhanden ist, bei dem die Menge des gebildeten Dianthracens wieder mit der Anfangskonzentration des Anthracens zunimmt und zwar ungefähr linear. Wir wollen dieses Gebiet C nennen. In diesem Gebiet C nimmt die Reaktionsgeschwindigkeit der Dianthracenbildung plötzlich und beträchtlich mit der Anfangskonzentration des Substrats zu. Übrigens steigt die gebildete Menge des Dianthracens in einem bestimmten Zeitintervall in diesem Gebiet mit der Temperatur viel stärker an als beim Gebiet B.

In diesen drei vereinzelten Teilen bildet sich das Dianthracen aus Anthracen durch den je nachdem verschiedenen Reaktionsmechanismus.

In Tabelle 2 und Fig. 2 zeigten sich wieder die Verläufe der Beziehungen zwischen der gebildeten Menge des Dianthracens und der anfangskonzentration des Anthracens bei gleichen Temperaturen und mit verschiedener Belichtungszeitdauer, und zwar nämlich 5.0, 7.0 und 10.0 Stunden. Dabei verhalten sich die Kurven fast analog wie in Fig. 1.

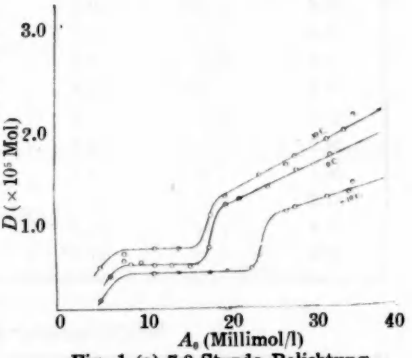

Fig. 1 (a) 7.0 Stunde Belichtung.

Übrigens haben wir die Messung der Quantenausbeute im Gebiet B unter Benutzung von 366$\mu\mu$ monochromatischem Licht vorgenommen. Die Ergebnisse sind in folgendem Abschnitt angegeben.

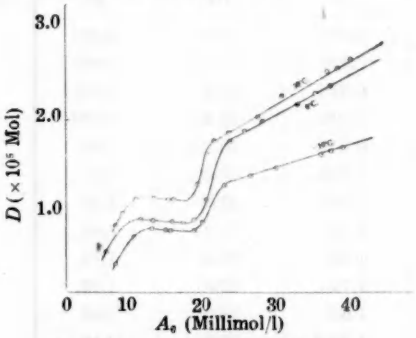

Fig. 1 (b) 5.0 Stunde Belichtung.

Quantenausbeute und Aktivierungsenergie. Die Quantenausbeute dieser Umsetzung im Gebiet B mit dem monochromatischen Licht von 366$\mu\mu$ ist folgenderweise zu bestimmen. Die gebildete Menge des Dianthracens in einer bestimmten Belichtungszeitdauer lässt sich durch die Umsatzmenge des Anthracens pro Zeiteinheit berechnen. Die Lichtmenge aus der monochromatischen Lichtquelle kann man durch die Forbeslösung[2] bestimmen, nachdem man die mit $KMnO_4$-Lösung titriert hatte.

(2) Leigton und Forbes, J. Am. Chem. Soc., **52** (1930), 3191.

Tabelle 1.

Die Menge des gebildeten Dianthracens aus der Anthracenlösung mit verschiedenen Anfangskonzentrationen.

Versuchstemperatur −10°C, 0°C und 30°C
Belichtungsdauer 7.0 Stunden

−10°C		0°C		30°C	
A_0	D	A_0	D	A_0	D
8.5	0.146	7.20	0.281	8.5	0.758
10.5	0.487	8.12	0.618	10.1	0.927
12.2	0.609	10.8	0.703	12.1	0.954
13.8	0.590	12.3	0.699	13.8	0.954
14.5	0.590	14.5	0.704	14.5	0.963
17.2	0.609	15.7	0.703	17.2	1.18
18.1	0.730	17.0	0.752	18.6	1.69
20.2	1.18	18.3	1.00	20.2	1.80
23.2	1.32	20.4	1.70	23.4	2.02
26.1	1.43	22.0	1.83	26.1	2.19
31.2	1.63	24.0	1.98	31.2	2.61
32.4	1.69	27.9	2.19	32.4	2.67
33.7	1.74	31.7	2.46	33.7	2.78

Belichtungsdauer 5.0 Stunden.

−10°C		0°C		30°C	
A_0	D	A_0	D	A_0	D
5.2	0.100	6.4	0.380	5.2	0.480
8.0	0.560	8.8	0.520	8.0	0.640
11.7	0.410	10.0	0.532	11.7	0.702
14.4	0.405	11.7	0.500	14.4	0.690
18.2	0.412	13.6	0.502	18.2	1.08
20.2	0.430	15.7	0.490	20.0	1.31
24.0	0.604	18.1	0.701	24.0	1.56
27.2	1.12	20.0	1.21	27.2	1.66
28.2	1.17	21.7	1.26	28.2	1.76
32.0	1.29	25.1	1.41	32.0	1.96
34.6	1.34	28.3	1.60	34.0	2.06
35.1	1.44	32.4	1.78	35.1	2.44

A_0: Anfangskonzent ation des Anthracens in Toluollösung in Millimol pro Liter.

D: Gebildete Menge des Dianthracens in 10^{-5} Mol.

Um über die Lichtabsorption der untersuchten Lösungen in verschiedenen Schichtdicken sowie auch über die Forbeslösung nähere Kenntnis zu erlangen, wurden die Messungen der Durchlässigkeit der genannten Flüssigkeit durchgeführt. Zu diesem Zwecke diente ein Photometer aus einer Vakuumphotozelle mit Innenschlag von Kalium mit Anschluss eines einstufigen Röhrenverstärkers. Um das Versuchsgefäss immer in gleicher Lage zu halten, wurde es in einen kleinen mit geeigneten Ausschnitten versehenen Aluminiumblock eingeschoben, in dem es durch ein Feder immer in gleicher Weise festgehalten wurde, mit Filter und Linsensystem versehene Beleuchtungslampe und das eingentliche Gehäuse der Photozelle

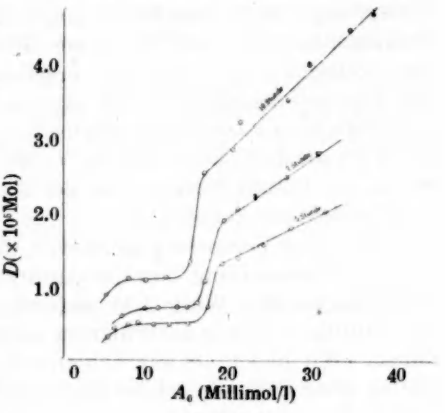

Fig. 2.

Tabelle 2.

Die Menge des gebildeten Dianthracens aus der Anthracenlösung in Toluol mit verschiedenen Anfangskonzentrationen und bei verschiedenen Belichtungszeitdauern.

Versuchstemperatur 0°C

5.0 Stunden.		7.0 Stunden.		10.0 Stunden.	
A_0	D	A_0	D	A_0	D
6.4	0.380	7.20	0.481	6.3	0.871
8.8	0.520	8.12	0.618	9.0	1.06
10.0	0.532	10.8	0.703	10.8	1.04
11.7	0.500	12.3	0.699	13.4	1.06
13.6	0.502	14.5	0.704	16.2	1.14
15.7	0.499	15.7	0.703	18.2	2.25
18.1	0.701	17.0	0.752	22.5	2.86
20.0	1.21	18.0	1.00	28.4	3.10
21.7	1.26	20.4	1.70	30.8	3.52
25.1	1.41	22.0	1.83	35.9	3.91
28.3	1.60	24.0	1.98	38.8	4.08
32.4	1.78	27.9	2.19		
		31.7	2.46		

A_0: Anfangskonzentration des Anthracens in Toluollösung in Millimol pro Liter.

D: Gebildete Menge des Dianthracens in 10^{-5} Mol.

eingesetzt. Das Versuchsgefäss stand hierbei senkrecht, die Schichtdicke der durchstrahlten Lösung wurde genau abgelesen. Die gute Übereinstimmung wiederholter Messungen bewies die Reproduzierbarkeit dieser Aufstellung. Auf diese Weise konnte man das Absorptionsvermögen der Anthracenlösung sowie auch der Forbeslösung bei den verschiedenen Schichtdicken und auch bei verschiedenen Konzentrationen bestimmen. Das Absorptionsvermögen der Anthracenlösung nimmt bei der kleinen Schichtdicke mit Zunahme derselben zu, aber es nimmt bald einen konstanten Wert an und unter unseren Versuchsbedingungen behält es durchaus seinen konstanten Wert der bei der ein wenig schwankenden Schichtdicke nicht wesentlich variiert.

Aus dem Versuche ging hervor, dass das Verhältnis der Lichtabsorption der Forbeslösung und die Anthracenlösung unter unseren Versuchsbedingungen den Wert 2.45 aufwies. Daraus kann man die Zahl J von der Anthracenlösung absorbierten Lichtquanten von $366\mu\mu$ pro Sek. berechnen. Wir haben als den Zahlenwert von $J=2.66\times10^{15}$. Das Verhältnis der in einer Sekunde gebildeten Dianthracenmolekülen D und der absorbierten Lichtquantenzahl J, also die Quantenausbeute bei verschiedenen Temperaturen ersieht man aus Tabelle 3. Dabei nimmt man als Zahlenwert der Quantenausbeute von der Forbeslösung 0.457 und wegen seines kleinen Tempraturkoeffizienten haben wir die Veränderung des oben geschriebenen Wertes mit der Temperatur ohne weiteres nachgelassen. Die Beleuchtung dauerte dabei immer 7.0 Stunden.

Nun können wir die von uns gewonnenen Zahlenwerte der Quantenausbeute etwas eingehender betrachten. Schon in der ersten Mitteilung haben wir darüber diskutiert, ob man im Gebiet B die Reaktionsgeschwindigkeit der Dianthracenbildung durch die Gleichung

$$\frac{dD}{dt} = k_1 A A' \qquad (1)$$

zum Ausdruck bringen soll, wo A bzw. A' die Konzentration des normalen bzw. angeregten Anthracenmoleküls und D die Zahl der gebildeten Dianthracenmoleküle vertritt. Nun ist der mittlere Zeitintervall, worin ein Quant von der Reaktionslösung absorbiert wird $1/J$, andererseits ist die mittlere Lebensdauer des angeregten Anthracenmoleküls $1/Z_{A'=1}$, wo $Z_{A'=1}$ die Gesamtstosszahl in einer Volumeinheit stattfindet, wodurch ein A'-Molekül entweder in die Dianthracenbildung oder in die Zurückverwandlung ins normale Anthracenmolekül eingeht. Daraus ergibt sich die Zahl $n_{A'}$ der A'-Molekül in cm.^{3},

$$n_{A'} = \frac{J}{VZ_{A'=1}}, \qquad (2)$$

wo V das Volum des Reaktionsgefässes ist. $Z_{A'=1}$ ist wieder proportional der Zahl der Stosspartner des A'-Moleküls d.h. der normalen Anthracenmoleküle und ist zu setzen

$$Z_{A'-1} = n_A Z_{A'-1,\,A-1}\,, \qquad (3)$$

wo $Z_{A'-1,\,A-1}$ bloss durch diese Gleichung zu definieren ist.

Die Gesamtzahl des normalen bzw. angeregten Anthracenmoleküle im Gefäss vom Volum V ist $n_A V$ bzw. $n_{A'} V$, und wir können hierbei auch mit recht annehmen, dass $e^{-\frac{E}{RT}}$ — ten Teil der normalen Anthracenmoleküle beim Zusammenstoss mit angeregten in die Reaktion zur Bildung von Dianthracen eingeht. Dann nimmt die Gleichung (1) die folgende Form an

$$\frac{dD}{dt} = k' Z_{A-1,\,A'-1} n_A V n_{A'} V \exp\left(-\frac{E}{RT}\right), \qquad (4)$$

wo k' eine Konstante und E die Aktivierungsenergie dieses elementaren Prozesses sind. R und T haben die übliche Bedeutung. Indem man die Ausdrücke (2) und (3) in (4) einsetzt, bekommen wir

$$\frac{dD}{dt} = k' V J \exp\left(-\frac{E}{RT}\right), \qquad (4')$$

und wenn man berücksichtigt, dass $\frac{dD}{dt}$ die Molekülzahl der pro Sek. umgesetzten Anthracenmoleküle ist, wird die Quantenausbeute φ dieser Umsetzung in diesem Gebiet

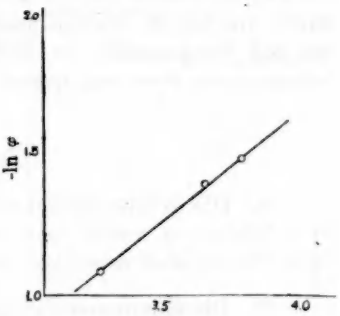

Fig. 3.

Tabelle 3.

Quantenausbeute der Photopolymerisation des Anthracens in Toluollösung mit einem monochromatischen Licht von 366$\mu\mu$.

Versuchstemperatur (°C)	$\frac{1}{T}\times 10^3$	Umgesetzte Menge des Anthracens. D Molekulzahl/Sek.	Quantenausbeute φ	ln φ
−10	3.802	5.83 10^{14}	0.219	−1.497
0	3.666	6.63 „	0.249	−1.399
30	3.301	9.01 „	0.338	−1.085

J: Die von der Anthracenlösung absorbierte Lichtquantenzahl von 366$\mu\mu$ pro Sek. $= 2.66\times 10^{15}$

φ: $\frac{D}{J}$

T: Absolut Temperatur.

$$\varphi = \frac{dD}{dt} \Big/ J = k' V \exp\left(-\frac{E}{RT}\right) \qquad (5)$$

und

$$\ln \varphi = k - \frac{E}{RT}, \qquad (5')$$

wo k wieder eine neue Konstante ist.

Aus dieser Formel kann man den Zahlenwert von E bei den verschiedenen Versuchstemperaturen berechnen, dessen Ergebnisse in Fig. 3 dargestellt wurde, wo $-\ln\varphi$ als Ordinate gegen $\frac{1}{T}$ als Abzisse aufgetragen. Daraus ersieht man, dass die Kurve geradlinig verläuft und aus ihrer Neigung erhält man die Aktivierungsenergie. Der daraus berechnete Zahlenwert von E betragt 1.75 Kal./Mol. Durch die Extrapolation der Kurve von Fig. 3 gewinnt man für den Zahlenwert der Quantenausbeute bei der Temperatur von 167° den Wert 0.44, der mit dem von Weigert bekommenen Wert gut übereinstimmt.[3]

Zusammenfassung.

1. Die Bildungsgeschwindigkeit des Dianthracens aus Anthracen in Toluollösung wurde noch weiter durchstudiert, und zwar bei verschiedener Temperatur sowie bei verschiedener Belichtungszeitdauer.

2. Die Quantenausbeute dieser Umsetzung mit monochromatischem Licht von 366$\mu\mu$ wurde bestimmt und aus der Benutzung des aus den Messungen gewonnenen Temperaturkoeffizienten haben wir den Wert von Weigert extrapoliert. Die beiden Werte erwiesen sich in guter Übereinstimmung.

Die vorliegende Untersuchung wurde durch das Stipendium der Ausgaben des Unterrichtministeriums für wissenschaftliche Forschung unterstutzt. Es ist mir eine angenehme Pflicht, Herrn Prof. Dr. Katayama für die wertvollen Hinweise zu danken. Bei den Messungen hat meine Assistentin Frl. T. Akimoto mitgearbeitet, wofür ich ihr auch hiermit danke.

Institut für physikalische Chemie der Toritsu-Hochschule, Tokio.

(3) Weigert, *Naturwiss.* **15** (1927), 124.

Étude biochimique sur les éléments des terres rares. I. Sur la distribution du néodyme dans les viscères.

Par Réinosuké HARA.

(Reçu le 21 février 1949.)

Introduction. Jusque'ici, les études systématiques sur la biochimie des éléments des terres rares ont été faites au laboratoire pharmacologique de l'université de Wurzburg[1] et de Florence.[2] Je pouvais obtanir le néodyme bien pur par la cristallisation fractionée en employant le nitrate de magnesium, et mettre à profit cette terre rare pour faire les présentes études systématiques. Ces études systématiques du néodyme ont été faites récemment par G. Guidi.[3] On a d'abord déterminé sa pureté au moyen de l'analyse spectroscopique à rayons X.

Les conditions de l'expérience sont comme suivante.

Appareil employé—type Siegbahn.
Cristal—Spath.
Courant électrique—5 mA.
Position du cliché—$N_d L_{\alpha 1}$, et $E_r L_{\alpha 1}$.
Tention électrique—15 KV.
Temps d'exposition—60 minutes.

Le résultat de l'analyse est montré dans la table 1.

Table 1.

position du cliché / ligne	Nd $L\alpha_1$	Er $L\alpha_1$
Nd $L\alpha_1$	###	
Nd $L\alpha_2$	##	
Nd $L\beta_1$	+	
Nd $L\beta_2$		###
Pr $L\alpha_1$	+	
Pr $L\alpha_2$	+	
Pr $L\beta_1$	±	
Pr $L\gamma_1$		±
La $L\beta_1$	±	
La $L\beta_2$	±	
Sm $L\alpha_1$	+	
Sm $L\beta_1$		±
Sm $L\gamma_1$		±

— très fort ## — assez fort
\+ — faible ± — très faible

Le néodyme employé contient la petite quantité de Pr, et les quantités minimum de Sm et de La. Cette expérience a été faite pour connaître certains mouvements du néodyme dans l'organisme. Autrefois, comme Guidi a étudié, l'absorption et l'évacuation du néodyme étaient très peu. Quand le néodyme est donné aux animaux par injection intra-

(1) S. Hara, *Arch. f. exper. Path.*, **100** (1923), 217 (Ce); H. Steidle et M. Ding, *Arch. f. exper. Path.*, **141** (1929), 273 (Y); H. Steidle et H. Dürr, *Arch. f. exper. Path.*, **145** (1929), 19 (Sm).

(2) M. Ajazzi-Mancini, *Arch. di. Fisiol.*, **24** (1926), 162; **25** (1927), 43, 257, 373 (La); P. Niccolini et G. Guidi, *Boll. Soc. ital. Biol. sper.*, **4** (1929), 1051 (La, Nd, Pr,); G. Guidi, *Arch. internat. Pharmacodynamie*, **37** (1930), 305; **39** (1930), 1 (Nd); P. Niccolini, *Arch. internat. Pharmacodynamie*, **37** (1930), 199 (Pr); P. Niccolini, *Arch. internat. Pharmacodynamie*, **40** (1931) 247 (Sm); P. Niccolini, *Boll. Soc. ital. Biol. sper.*, **6** (1931), 202, 204; **7** (1932), 998 (Nd. Pr. Sm).

(3) G. Guidi, *Arch. internat. Pharmacodynamte*, **37** (1930), 305; **39** (1931), 1.

veine, intramuslaire, on ne peut jamais trouver cet élément dans l'évacuation. J'ai examiné le mouvement de cet élément dans l'organisme au moyen de l'analyse spectroscopique à rayons X.

Expérience. animal– le rat, au poids du corps de 70–100g.
Conditions de l'expérience. D'après G. Guidi,[4] en la solution à 1.666% chlorure du néodyme est isotonique contre le sang, et d'après L.C. Maxwell,[5] le dose mortelle du chlorure du néodyme aux rats est 30-40mg./kg. en injection intraveine. J'ai injectioné 0.2c.c. de la solution du chlorure du néodyme à 1.5% une fois par jour pendant deux jours. Cinq jours après, on a dissequé le rat et a confirmé par l'analyse spectroscopique à rayons X. Les conditions de cette analyse sont mêmes que la détermination de la pureté.

Table 2.

		NdLα_1	NdLα_2	NdLβ_1	Pr Lα_1	Pr Lβ_1			NdLα_1	NdLα_2	NdLβ_1	Pr Lα_1	Pr Lβ_1
foie	1	⫴	+	+	±	±	cœur	1	±				
	2	+	+	+				2	±				
	3	⫴	+	+	±	±		3					
	4	⫴	+	+	±			4	+	±	+		
	5	⫴	+	+	±	±		5	±				
rate	1	+	+	+			poumon	1	⫴	+	+	±	
	2	⫴	+	+	±			2	+	±	+		
	3	⫳	+	⫴	+	±		3	+	±	±		
	4	⫴	+	+				4	+	±	±		
	5	⫴	+	+	±	±		5	+	±	±		
rein	1							1	+	±			
	2	±					estomac, intestin	2	+	±	+		
	3	±					et	3	+	±	+		
	4						leurs contenus	4	+	±	+		
	5	±						5	+	±	+	±	±
pancréas	1						"1,2,3,4,5" indiquent les numéros des animaux.						
	2												
	3						⫳ — très fort ⫴ — assez fort						
	4	±					+ — faible ± — très faible						
	5												

(4) G. Guidi, *Arch. internat. Pharmacodynamie*, **37** (1930), 306.
(5) L. C. Maxwell et F. Bischoff, *J. Pharmacol.*, **43** (1931), 61.

Les resultats de l'analyse spectroscopique à rayons X sont montrés dans la table 2.

Mêmes après cinq jours d'injection, on peut trouver une très grande quantité de ce sel dans chaque viscère, et sur cinq rats, dans le foie et la rate, la ligne Nd$L\alpha_1$ qui est la ligne de la mise évidence est presque toujours forte ou assez forte, et on peut trouver aussi les lignes Nd $L\alpha_2$, Nd $L\beta_1$, et les lignes Pr $L\alpha_1$, Pr $L\beta_1$. On peut trouver la ligne Nd $L\alpha_1$ et de plus les lignes Nd $L\alpha_2$, Nd $L\beta_1$ au poumon. On n'a pas trouvé la ligne Nd $L\alpha_1$ aux pancréas, rein, et cœur, ou si on l'a trouvée, l'intensité du Nd $L\alpha_1$ est négligeable. Dans l'estomac, l'intestin, et leurs contenus, on a trouvé les lignes Nd $L\alpha_2$, Nd $L\beta_1$ autre de la ligne Nd $L\alpha_1$, et pour un seul cas, les lignes Pr $L\alpha_1$ et Pr $L\beta_1$.

Concentration du néodyme dans l'évacuation. Pour cinq rats, on a decomposé toute évacuation de sept jours dans le flacon Kjeldahl par l'acide sulfurique et par l'acide azotique. On a ensuite ajouté l'acide chlorhydrique pour dissoudre sulfate du calcium. Par l'addition d'hydroxyde du natrium, en obtenant le précipité d'hydroxyde, on l'a fait dissoudre dans l'acide chlorhydrique, et ajouté 5mg. du chlorure du cérium (excempt des Nd, La, Sm). On a alors obtenu le précipité enduit par l'acide oxalique et procédé l'analyse spectroscopique à rayons X après la calcination de ce précipité. Les résultats de l'analyse sont montrés dans la table 3.

Table 3.

Nd $L\alpha_1$	Nd $L\alpha_2$	Nd $L\beta_1$
⫼	+	⫫

Conclusion. (1) En donnant le sel du néodyme à l'organisme, il change au certain composé insoluble, se dépose dans chaque viscère et son évacuation est très peu remarquable. C'est-à-dire même après cinq jours d'injection, on peut trouver très grande quantité de ce sel au chaque viscére et ne peut trouver dans l'évacuation au moyen de l'analyse spectroscopique à rayons X.

(2) En un mot, les viscères dans lesquels se dépose le sel sont phagocyte, tels le sytème réticulendothériale et la cellule épithériale du poumon. Sur cinq rats, le sel a été trouvé remarquablement dans le foie et la rate. On peut aussi trouver le sel dans le poumon.

(3) Les viscères ôu le sel ne se dépose guère sont le pancréas, le rein, et le cœur.

(4) L'analyse spectroscopique à rayons X pour l'évacuation des cinq rats a donné les résultats suivants. La ligne Nd $L\alpha_1$ est forte, on a trouvé aussi les lignes Nd $L\alpha_2$, Nd $L\beta_1$, mais leurs intensités sont plutôt faibles pour sept jours d'évacuation.

À la fin de ce compte-rendu, je devoué mes reconnaissances plus profondes à M. le Prof. Kenjiro Kimura pour les instructions extrêmement soigneuses.

Laboratoire de Chimie minérale, Faculté des Sciences, Université de Tokyo.

The Reaction of Aluminum Sulfate and Calcium Carbonate. I. Preparation of Basic Aluminum Sulfate Sol and its Hydrolysis

By Tsutomu KUWATA and Tadahisa NAKAZAWA

(Received March 12, 1949.)

Introduction. It has been known that basic aluminum sulfate may be produced by dissolving aluminum hydroxide in aluminum sulfate solution. The solubility of the oxide measured by R. Kremann, K. Hüttinger[1] was relatively small at room temperature and the ratio of Al_2O_3: SO_3 is about 1 mol:2 mol. N. Grüstein[2] has claimed in his patent that pure aluminum hydroxide is prepared by the hydrolysis of basic aluminum sulfate solution containing ferrous sulfate. The solution was produced by reacting iron powder on the concentrated solution of aluminum sulfate containing iron salts. Another patent claimed by G.H. Hultman[3] is that the pure basic aluminum sulfate is precipited by calcium carbonate from the dilute solution of aluminum sulfate and ferrous sulfate.

If we assume that the reaction of calcium carbonate and aluminum sulfate is as follows,

$$Al_2(SO_4)_3+3CaCO_3+3H_2O=2Al(OH)_3+3CaSO_4+3CO_2,$$

3 mols of $CaCO_3$ are necessary for 1 mol of $Al_2(SO_4)_3$. But the reaction is neither so simple nor so perfect.

Change of the Composition of Aluminum Sulfate Solution with the Amount of Reacting Calcium Carbonate. In this experiment a known amount of calcium carbonate in milky state was added little by little in 100c.c. of aluminum sulfate solution under a vigorous agitation in the course of 4–5 hrs. An unvigorous agitation or a quick addition of calcium carbonate is unfavorable for the reaction, because they often induce the formation of large crystals of calcium carbonate or the covering of the carbonate with small crystals of calcium sulfate.

After the whole amount of calcium carbonate was added, the agitation was continued for 30 minutes, and then the precipitate was filtered. The analysis of the filtrate was carried out in the usual manner:i.e. Al_2O_3 by the gravimetric method and SO''_4 by the volumetric method using benzidin hydrochloride as the precipitation agent. The pH of the filtrate was observed by the test paper.

(1) R. Kremann, K. Hüttinger, *Jahresb. Geol. Reichsanst., Wien*, **58**, 637, (1908).
(2) N. Grünstein, Brit. P., 472, 229 (1937).
(3) G. H. Hultman., U. S. P. 1,607,279 (1926).

Table 1.
The relation between the amount of the reacted carbonate and the composition of the filtrate.

No.	$CaCO_3$ add. % to equivalent	Al_2O_3 concn		SO_3 concn.		SO_3/Al_2O_3 molar ratio
		g./c.c.	% to original concn.	g./c.c.	% to original concn.	
Solution I	—	0.0856	100	0.2040	100	2.97
1	60.0	0.0879	102.7	0.1021	50.1	1.47
2	75.0	0.0355	41.5	0.0392	19.3	1.33
3	89.9	0	0	0.0035	1.7	—
4	99.9	0	0	0.0018	0.9	—
Solution II	—	0.1178	100	0.2810	100	3.03
1	58.6	0.1221	103.6	0.1613	57.5	1.68
2	76.2	0.1205	102.2	0.1262	44.9	1.33
3	93.9	0.0521	44.2	0.0525	18.7	1.28
4	117.3	0	0	0.0043	1.6	—
Solution III	—	0.1231	100	0.2758	100	2.85
1	59.9	0.1288	104.6	0.1651	60.0	1.63
2	74.5	0.1316	106.9	0.1218	44.3	1.18
3	85.5	0.1274	103.5	0.1103	40.1	1.10
4	99.3	0.0516	41.9	0.0533	19.3	1.31

The Solutions II and III correspond to the saturated solution at ca. 20° and 38–40°C respectively.

In the above table, some data which overrun from the original concentration of Al_2O_3 wouuld be accounted for the concentration of the solution being taken off some water for the crystallization of calcium sulfate. The results obtained are shown in Fig. 1.

While the concentration of SO''_4 decreases linearly in proportion to the amount of the $CaCO_3$ added, the aluminum content in the solution does not decrease in the same manner and the more concentrated solution can retain more aluminum in the solution. As a result, highly basic aluminum sulfate sol may easily be obtained from the concentrated solution of aluminum sulfate by this process.

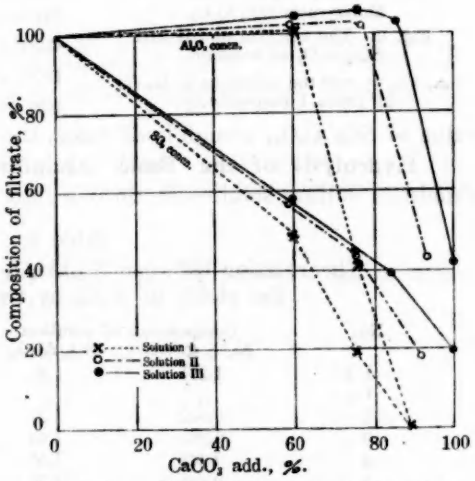

Fig. 1. The relation of the amount of reacted $CaCO_3$ and the composition of the filtrate.

The reaction of $CaCO_3$ with the solution of aluminum sulfate, however, is somewhat delicate. If the addition of $CaCO_3$ is too quick, an insoluble form of basic aluminum sulfate deposits with $CaSO_4$. In such a

case, the decrease of molar ratio SO_3/Al_2O_3 of the solution stops at an unsatisfactory extent. It is also interesting that the small overcharge of calcium carbonate causes the almost perfect precipitation of the insoluble basic aluminum sulfate.

Sol-Gel Transformation. The concentrated and highly basic aluminum sulfate solutions, like solutions II-No. 3 in Table 1, are viscous and transparent with a faint blue fluorescence. They are relatively stable and unvariable for the stock of several months at room temperature, although some samples deposit, in these standings, the white fairly dense precipitates. When the stable and highly basic aluminum sulfate solutions are heated up to 50-70°C, they coagulate to opaque gelatineous gels. Since this sol-gel transformation is reversible according to temperature, it again changes to the original sol form when standing at room temperature. This remarkable phenomena of highly basic aluminum sulfate solution is assumed to be accounted for the change of hydration degree of associated aluminum hydroxysulfate molecules. The details are left for a future study.

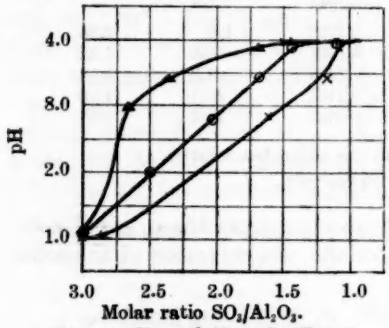

Fig. 2. The relation of pH and SO_3/Al_2O_3 of solution.
△, ○, × are the solutions I, II, III in Table 1 respectively.

pH of the Basic Aluminum Sulfate. The relation of pH and molar ratio SO_3/Al_2O_3 of the basic aluminum sulfate solution is not definite. It differs with the concentration of Al_2O_3. The more dilute solution of basic aluminum sulfate shows the larger value of pH at the same value of SO_3/Al_2O_3, though in all cases, the pH becomes about 4.0 after all.

Hydrolysis of the Basic Aluminum Sulfate. When the basic aluminum sulfate solution is thrown into water, a while precipitate is

Table 2.
The relation between SO_3/Al_2O_3 of the solutions and the yields of Al_2O_3 by their hydrolysis.

No.	Composition of solution Al_2O_3 g./c.c.	SO_3/Al_2O_3	Yield of the precipitate (observed as Al_2O_3) %
1-1	1.274	1.10	79.8
1-2	,,	,,	81.4
2	0.502	1.27	64.9
3	0.282	1.44	57.6
4	0.202	1.58	52.9
5	0.125	1.73	52.0

No. 1-2 was thrown into the water at 20°C. and not heated.

readily produced. This precipitate is a kind of basic aluminum sulfate having the molar ratio $Al_2O_3:SO_3=1:0.5–0.6$. It corresponds to the com-

The concentration of solution observed as Al_2O_3 g/c.c.: (1) 0.0501, (2) 0.104 (3) 0.123

position of $2Al_2O_3 \cdot SO_3 \cdot xH_2O$. It is fairly dense and can easily be filtered.

Five c.c. of the basic aluminum sulfate are thrown into 50 c.c. of water at 80°C. and well stirred and then filtered. The relation of SO_3/Al_2O_3 of the basic aluminum sulfate and the yield of the precipitate are shown in Table 2. and Fig. 3.

It seems that in spite of the distinction of the concentration of the basic aluminum sulface solution, the yield of Al_2O_3 is in a linear relation with SO_3/Al_2O_3 of the basic solution.

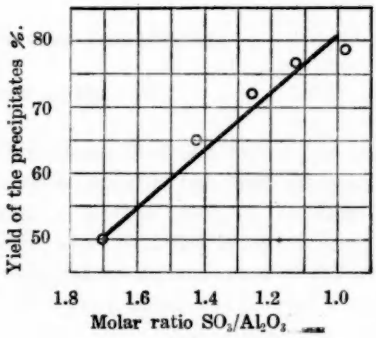

Fig. 3.

The preparative method of aluminum hydroxide or alumina studied by the present authors is also of much interest for the separation of aluminum and iron from their sulfate solution, because ferrous sulfate does not show such hydrolytic change.

Summary

1. By the moderate reaction of calcium carbonate and the concentrated solution of aluminum sulfate, highly basic aluminum sulfate sol is easily obtained.

2. Some kinds of the basic aluminum sulfate sol become gel on heating and the sol-gel transformation is perfectly reversible at the neighbourhood of 40-50°C.

3. On dilution with water, the highly basic aluminum sulfate (SO_3/Al_2O_3=1.1–1.6) hydrolyses and precipitates the insoluble basic aluminum sulfate ((SO_3/Al_2O_3=0.5–0.6).

A part of this study was assisted by Mr. Hiromichi Asai, to whom the authors wish to express their thanks.

Department of Applied Chemistry,
Faculty of Engineering,
University of Tokyo